Induction of tolerogenicity following a molecular dialogue between HTLV-1-infected T cells and dendritic cells

Auriane Carcone[1], Franck Mortreux[2], Sandrine Alais[1], Cyrille Mathieu[3], Chloé Journo[1,#], Hélène Dutartre[1,#]*

Affiliations:

[1] Centre International de Recherche en Infectiologie, Retroviral Oncogenesis, Inserm U1111 - Université Claude Bernard Lyon 1, CNRS, UMR5308, Ecole Normale Supérieure de Lyon, Université Lyon, Lyon, France.

[2] Laboratory of Biology and Modelling of the Cell, University of Lyon, ENS de Lyon, University Claude Bernard, CNRS UMR 5239, Inserm U1210, Lyon, France.

[3] Centre International de Recherche en Infectiologie, équipe Neuro-Invasion, TROpism and VIRal Encephalitis, Inserm U1111 - Université Claude Bernard Lyon 1, CNRS, UMR5308, Ecole Normale Supérieure de Lyon, Université Lyon, Lyon, France.

# Equal contribution

* Corresponding author

Abstract

Manipulation of immune cell functions, independently of direct infection of these cells, emerges as a key process in viral pathophysiology. Chronic infection by Human T-cell Leukemia Virus type 1 (HTLV-1) is associated with immune dysfunctions, including misdirected responses of dendritic cells (DCs). Here, we interrogate the ability of HTLV-1-infected T cells to indirectly manipulate human DC functions. We show that upon coculture with chronically infected T cells, monocyte-derived DCs (MDDCs) fail to fully mature. We further show that exposure to HTLV-1-infected T cells induces a unique transcriptional signature in MDDCs, which differs from a typical maturation program, and which is correlated with a dampened ability of HTLV-1-exposed MDDCs to subsequently respond to restimulation. Induction of this tolerogenic behavior is not strictly dependent on capture of HTLV-1 viral particles by MDDCs, nor on cell-cell contacts between HTLV-1-infected T cells and MDDCs, but is instead the result of a molecular dialogue between HTLV-1-infected T cells and MDDCs upon coculture, illustrating how HTLV-1 might indirectly induce a local tolerogenic immune microenvironment suitable for its own persistence.

Introduction

Chronic infection by the deltaretrovirus Human T-cell Leukemia Virus type 1 (HTLV-1) generally remains asymptomatic, but leads to severe diseases in 5 to 10% of infected individuals[1], in the form of Adult T-cell Leukemia/Lymphoma (ATL), or Tropical Spastic Paraparesis/HTLV-1 Associated Myelopathy (TSP/HAM). Remarkably, HTLV-1 chronic infection increases the risk of viral, bacterial or parasitic co-infections[2]. In agreement with these clinical observations, immune dysfunctions have been repeatedly reported in asymptomatic HTLV-1 carriers, years before severe diseases were diagnosed, indicating that chronic infection induces systemic effects and impairs the ability of the immune system to

respond appropriately to infectious and non-infectious triggers[3–7]. Dendritic cells (DCs) are critical mediators of innate and adaptive immune responses during viral infection. Upon efficient viral recognition, DCs undergo a maturation program that renders them capable of inducing specific T-cell responses. The DC maturation process is characterized by a transcriptional program that translates, among others, in the upregulation of several maturation markers at the cell surface (*e.g.* CD80, CD86), accompanied by the secretion of pro-inflammatory cytokines such as tumor necrosis factor alpha (TNF-α), and antiviral cytokines such as type I interferons (IFN-I)[8]. However, inappropriate DC responses can contribute to immunopathology, a process that is exacerbated in chronic viral infections[9].

The role of DCs in HTLV-1 infection has been extensively investigated in terms of viral transmission to $CD4^+$ T cells, both *in vitro*[10–12] and in animal models[13,14]. Whether HTLV-1 induces the maturation of DCs has been investigated *in vitro*, but only using murine bone marrow-derived DCs exposed to cell-free Moloney-pseudotyped chimeric HTLV-1[15]. Given that cell-free HTLV-1 is not detected in HTLV-1 carriers or patients, *in vivo* DCs are probably mostly exposed to chronically infected cells rather than cell-free virus. Hence, these experimental settings may not fully recapitulate *in vivo* virus / host interactions.

Strikingly, myeloid cells such as monocytes and DCs can harbor infectious HTLV-1 genomes in infected individuals, including in asymptomatic individuals[6,16], and exhibit impaired phenotypes and functions[16–18] that may correlate with their proviral load[19]. These observations in humans indicate that HTLV-1 could in fact dampen the responsiveness of infected DCs, which may ultimately contribute to immune dysfunction during chronic infection. Accordingly, DCs derived from ATL patients exhibit maturation defects[17] associated with an inability to induce proliferation of $CD4^+$ T cells[18]. However, because the proportion of DCs infected *in vivo* is low, the impact of HTLV-1 on DC function might not be solely attributed to HTLV-1-infected DCs, suggesting that HTLV-1 could indirectly modulate the functions of

DCs, in the absence of direct infection. In this work, we aimed at determining whether HTLV-1 transformed T cells could indirectly affect human DC functions *in vitro*. In contrast with previous work using murine cells and cell-free virus, we show that upon coculture with HTLV-1 transformed T cell lines, human monocyte-derived DCs (MDDCs) do not fully mature. We further show that exposure to HTLV-1-infected T cells induces a unique transcriptional signature in MDDCs, which differs from a typical maturation program, and which is correlated with a dampened responsiveness of HTLV-1-exposed MDDCs to subsequent stimulation. Interestingly, this tolerogenic behavior is induced as the result of a molecular dialogue between HTLV-1-infected T cells and MDDCs upon coculture. This unique mechanism of viral-induced tolerance in DCs illustrates how HTLV-1 might indirectly manipulate innate cells to induce a local immune microenvironment suitable for its own persistence.

Results

Human MDDCs do not fully mature when exposed to HTLV-1-infected T cells

To determine whether chronically infected T cells could directly or indirectly manipulate human DC functions *in vitro*, we first addressed whether infected T cells were sensed by DCs. We used human monocyte-derived DCs (MDDCs) cultured *in vitro* with HTLV-1-infected and transformed T cell lines, and assessed MDDCs maturation by flow cytometry after 24h or 48h of coculture, using the MDDC-specific CD11c marker to identify MDDCs in the coculture (see **Fig. 1a** for the experimental settings, **and Supplementary Fig. 1** for the gating strategy). At these time points, less than 1% of MDDCs have integrated the viral genome and they do not release virions[11], indicating that they are not productively infected. In contrast to MDDCs exposed to measles virus (MeV), MDDCs exposed to HTLV-1 transformed C91-PL cells, failed to fully upregulate CD86, used in this first experiment as a surrogate of DC maturation (**Fig. 1b, left panel**). Repeated experiments using MDDC samples from independent donors showed that while around 90% of MDDCs upregulated CD86 upon exposure to MeV, regardless of their ability to express MeV (**Fig. 1b, right panel**, compare total versus GFP^- and GFP^+ MDDCs), as well as upon stimulation by the TLR-4 agonist LPS (**Fig. 1b, right panel**), the percentage of activated MDDCs after coculture with HTLV-1-transformed C91-PL cells remained low (**Fig. 1b, right panel**). To exclude a cell line-specific effect, and to thoroughly characterize MDDCs maturation status, MDDCs were exposed to several control uninfected T cell lines (**Supplementary Fig. 2a-f**; Jurkat, CEM or Molt-4 T cell lines, green bars), as well as to several HTLV-1-transformed T cell lines (**Supplementary Fig. 2a-f**; C91-PL, MT-2 or Hut102; blue bars), and the regulation of both maturation markers CD86, CD83, CD80, and CD40, (**Supplementary Fig. 2a-d**) and inhibition markers ICOSL and PD-L1 (**Supplementary Fig. 2e-f**) at the cell surface was

monitored by flow cytometry. All the HTLV-1-transformed T cell lines induced either no change, or only minor changes, in the expression (percentage of positive cells and normalized mean signal intensity, MFI) of maturation or inhibition markers at the surface of cocultured MDDCs (**Supplementary Fig. 2a-f**). Increasing the duration of coculture to 48h did not impact these observations (**Supplementary Fig. 2a-f**), excluding a delay in maturation. The inefficient upregulation of MDDC maturation markers was also accompanied by a low ability to secrete TNF-α or IFN-I (**Fig. 1c** and **Supplementary Fig. 2g**), strengthening the notion that HTLV-1-infected T cells do not induce a typical maturation program in MDDCs, and thus might not be efficiently sensed by human DCs, in contrast to observations made with cell-free virus in a mouse model[15]. Since similar observations were made with all HTLV-1-infected T cell lines tested, and with the tested maturation markers and cytokines, only the C91-PL T cell line and CD86 were used in some of the following experiments.

Previous work from our laboratory showed that MDDCs efficiently capture HTLV-1 after coculture with HTLV-1-infected T cell lines[11], suggesting that in our experimental conditions, HTLV-1 capture itself is inefficient in driving MDDC maturation. To formally demonstrate this, we assessed HTLV-1 capture in MDDCs following coculture, by staining the HTLV-1 Gag p19 structural protein. As expected, MDDCs were efficient at capturing HTLV-1 (**Fig. 1d**), irrespective of the infected T cell line used in the coculture (**Supplementary Fig. 2h**), with around 30% of capture observed in a representative coculture experiment with C91-PL cells (**Fig. 1d, left**), and reaching up to 80% of capture observed in repeated experiments using independent donors (**Fig. 1d, right**). Maturation was then compared in MDDCs that had not captured HTLV-1 (Gag p19-negative MDDCs, cyan, **Fig 1e**), or had captured HTLV-1 (Gag p19-positive MDDCs, magenta, **Fig. 1e**). Although CD86 expression was consistently higher in p19-positive MDDCs (**Fig. 1e**, **right**, compare cyan and magenta bars), the percentage of Gag p19-positive cells remained low compared to fully matured LPS-exposed

MDDCs (**Fig. 1e**, compare magenta and red bars), highlighting that maturation remained inefficient even in MDDCs that had capture HTLV-1. No significant correlation was detected among repeated experiments between the level of HTLV-1 capture and the efficiency of MDDC maturation (**Supplementary Fig. 2i**, $p = 0.1412$), further confirming that HTLV-1 capture itself is inefficient in driving MDDC maturation.

Taken together, these observations, recapitulated in **Fig. 1f**, demonstrate that cell-associated HTLV-1 fails to fully mature MDDCs, suggesting that it is poorly sensed by these human innate cells.

Exposure to HTLV-1-infected T cells induces a unique transcriptional signature in MDDCs

Interestingly, our previous work demonstrated that in contrast to MDDCs, plasmacytoid dendritic cells (pDC) do efficiently sense cell-associated HTLV-1[20]. Inefficient sensing of HTLV-1-infected T cells by MDDCs could be the result of either a stealth behavior of cell-associated virus towards MDDCs, resulting in a *bona fid*e lack of response specifically in this cell type, or, alternatively, to the active manipulation of MDDC functions by HTLV-1-infected T cells, resulting in a specific response that differs from a typical maturation program. To discriminate between both these scenari, we aimed at determining the complete transcriptomic landscape of MDDCs after exposure to HTLV-1-infected T cells, or to control uninfected T cells, using bulk RNA-seq (**Fig. 2**). After 24h of coculture, MDDCs were magnetically separated from C91-PL or control Jurkat T cells, based on the exclusive expression of CADM1 on T cells (**Supplementary Fig. 3a**). Note that although the levels of CADM1 were higher at the surface of C91-PL cells compared to Jurkat cells (**Supplementary Fig. 3a**), a similar MDDC enrichment yield of around 99 % was observed after separation in both conditions, with no significant T cell contamination (**Supplementary**

Fig. 3b). LPS-stimulated MDDCs were also included in the RNA-seq analysis, as a reference for fully matured MDDCs. RNA was extracted from each MDDC sample, and submitted to quality control followed by sequencing.

First, to show global similarities in gene expression between samples, unsupervised hierarchical clustering and principal component analysis (PCA) were performed on normalized transcript count tables. Analysis of sample clustering along the two first PCs (**Fig. 2a,** PC1 and PC2), that explain 81 and 8% of the total variance, respectively, showed that the main source of variance in the dataset was the stimulation by LPS, followed by the infection status of cocultured T cells, while the identity of the MDDC donor contributed only weakly to the global variance. In agreement with flow cytometry data shown in Fig. 1, this confirmed, at the transcriptional level, the inefficient activation of MDDCs after exposure to HTLV-1-infected T cells, which contrasts with the typical maturation program of fully activated MDDCs. This also indicates that exposure to HTLV-1-infected T cells does induce a detectable, yet subtle, transcriptional response, when compared to exposure to uninfected T cells.

To characterize the changes in gene expression in MDDCs induced by exposure to HTLV-1-infected T cells, we used DESeq2 to identify differentially expressed genes (DEGs) between C91-PL- and Jurkat-exposed MDDCs. As a reference for a typical maturation program, we identified DEGs between LPS- and Jurkat-exposed MDDCs. Using a fold-change cut-off of 2, a total number of 474 DEGs were obtained between C91-PL- and Jurkat-exposed MDDCs ($padj<0.05$), with 435 genes found significantly upregulated upon HTLV-1 exposure, and 39 genes found significantly downregulated (**Fig. 2b** and **Supplementary Table 1**). A heatmap of the 474 DEGs showed clustering between samples, as expected (**Supplementary Fig. 4a**).

To gain insight into the processes modulated in MDDCs after exposure to HTLV-1-infected T cells, we performed gene ontology analysis on the set of 435 upregulated genes. Over-

represented KEGG pathways were retrieved and filtered to reduce redundancy (see **Supplementary Table 2**), leading to a final list of 7 pathways (**Fig. 2c** and **Supplementary Tables 2 and 3**). Strikingly, exposure to HTLV-1-infected T cells was characterized by significant over-representation of upregulated genes involved in lipid biosynthesis and metabolism (**Fig. 2c**). Interestingly, genes involved in several pathways linked with response to viral infection were also over-represented, including genes involved in innate immune sensing (sub-pathways: RIG-I or Toll-like receptors and NOD-like receptors), in viral infection (sub-pathways: Influenza A, Measles, Hepatitis C, Hepatitis B, Human Papillomavirus, Herpes simplex virus 1, Coronavirus, HIV, EBV), and in the NF-κB signaling pathway. Taken together, these results confirm that exposure to HTLV-1-infected T cells does induce a transcriptional response in MDDCs, indicating that sensing does occur to some extent, but does not culminate in a typical maturation and anti-viral program.

To further determine the extent to which this transcriptional response is distinct from a typical maturation signature, we compared the genes affected by LPS stimulation of Jurkat-exposed MDDC to those affected by MDDC exposure to C91-PL. Among the 474 DEGs, 373 genes were also differentially expressed after LPS stimulation (**Fig. 2d**), representing only 5% of all LPS-modulated genes. Among these shared genes, 7 genes annotated as involved in the NF-κB signaling pathway were retrieved, including *CCL19, TNFSF13B, TRIM25, BCL2L1* and *BCL2A1* (**Supplementary Fig. 4b**). However, the level of up-regulation of these shared NF-κB-related genes was strikingly lower after HTLV-1 exposure compared to LPS stimulation (**Supplementary Fig. 4b**)**.** This observation of a lower magnitude of differential expression (either up- or downregulation) was general to most of the 373 shared DEGs (**Fig. 2e**)**.** Of note, the *RELA, RELB* and *NFKB1* genes that were upregulated by LPS stimulation were not upregulated upon C91-PL exposure (**Supplementary Fig. 4c**), possibly contributing to the lower activation of the NF-κB-dependent genes observed above (**Supplementary Fig. 4b**). In

addition, among the 377 Interferon-Stimulated Genes (ISG) listed in **Supplementary Table 1**, only 121 were retrieved in the set of significantly upregulated genes, and again, their up-regulation was lower to that induced by LPS stimulation (**Supplementary Fig 4d**). These observations strengthen the notion that while sensing of HTLV-1-infected T cells does occur to some extent, the magnitude of the maturation and antiviral transcriptional response remains very limited, which is consistent with the inefficient maturation of MDDCs observed at the protein level (see **Fig. 1**).

Interestingly, among the 474 DEGs, 101 genes were not present in the list of DEGs between LPS- and Jurkat-exposed MDDCs (**Fig. 2d and f**), defining a unique transcriptional signature associated with the exposure to HTLV-1-infected C91PL cells. Due to the limited number of genes included in this specific signature, gene ontology analysis was not feasible. Interestingly however, several genes retrieved in Fig. 2c as those involved in lipid biosynthesis and metabolism, were also included in this specific signature, such as *ELOVL3* (Elongation of Very Long Fatty Acid Elongase 3), *FADS1* (Fatty Acid Desaturase 1), and *SLC27A6* (Solute Carrier Family 27 Member 6, a member of the fatty acid transport protein family) (**Fig. 2g**). Altogether, these transcriptomic analyses demonstrate that exposure to HTLV-1-infected T cells is not completely silent in MDDCs, but rather results in a unique transcriptional response that differs from a typical maturation program. This supports the notion that HTLV-1-infected T cells might actively manipulate MDDC functions to limit their functional response, possibly by rewiring lipid biosynthesis and metabolism.

Pre-exposure to HTLV-1-infected T cells dampens the responsiveness of MDDCs to subsequent stimulation

We next aimed at investigating whether this unique transcriptional response observed upon exposure to HTLV-1-infected T cells indeed translates into functional defects in MDDCs,

beyond their inefficient maturation. To this end, we addressed whether pre-exposure to HTLV-1-infected cells influenced MDDC responsiveness when exposed to a subsequent stimulation. After 24h of coculture with HTLV-1-infected T cell lines, MDDCs were restimulated with strong inducers of MDDCs maturation, in the form of LPS (TLR-4 ligand) or R848 (TLR-7/8 ligand, **Fig. 3a**), for another 24h. When compared to MDDCs pre-exposed to uninfected control T cell lines (red bars), MDDCs pre-exposed to HTLV-1-transformed T cells (dark blue bars) upregulated CD86 (as well as other maturation markers) to a significantly lower extent when stimulated by LPS or R848 (**Fig. 3b, Supplementary Fig. 5a-d**). In addition, TNF-α secretion by MDDCs upon LPS stimulation was also significantly reduced by pre-exposure to HTLV-1-transformed T cells (**Fig. 3c**, left panel, **Supplementary Fig. 5e**), while IFN-I secretion was not affected (**Fig. 3c**, right panel, **Supplementary Fig. 5e**). These results indicate that pre-exposure to HTLV-1-transformed T cells indeed influences the responsiveness of MDDCs to subsequent stimulation, by specifically dampening their pro-inflammatory response (monitored here through the upregulation of maturation markers and through TNF-α secretion), without hampering their antiviral response (monitored here through IFN-I secretion) (recapitulated in **Fig. 3d**). This suggests that HTLV-1 might specifically manipulate the responsiveness of certain signaling pathways in MDDCs, such as the NF-κB pathway upstream of the pro-inflammatory program, while leaving the responsiveness of others unaffected, such as the IRF3 pathway upstream of the antiviral program.

Pre-exposure to HTLV-1-transformed T cells alters the transcriptional response of MDDCs to subsequent stimulation

To obtain a broader overview of how pre-exposure to HTLV-1-transformed T cells affects the responsiveness of MDDCs, a second bulk RNA-seq analysis was conducted on MDDCs pre-

exposed to an HTLV-1-infected T cell line (C91-PL), or to a control uninfected T cell line (Jurkat), and then restimulated by LPS (**Fig. 4**). To address whether viral capture was required for this manipulation of MDDC responsiveness, we also included in the RNA-seq analysis MDDCs cocultured with the HTLV-1-infected C8166 T cell line that does not produce viral particles[21]. As expected, no viral particle was captured by C8166-exposed MDDCs, in contrast to C91-PL-exposed MDDCs (**Supplementary Fig. 6**).

PCA analysis of samples showed that both the donor and the infection status of cocultured T cells were the main sources of variance in the dataset (**Fig. 4a**), confirming that pre-exposure to HTLV-1-transformed T cells does alter the transcriptional response of MDDCs to subsequent stimulation. In contrast, the ability to capture HTLV-1 did not contribute to a visible extent to the global variance, suggesting that viral capture might not be required for this alteration.

We then retrieved the lists of genes differentially expressed between the different experimental conditions. In agreement with the PCA analysis, 1324 genes were found differentially expressed between LPS-stimulated C91-PL-pre-exposed MDDCs, and LPS-stimulated Jurkat-pre-exposed MDDCs (**Supplementary Table 4**), with a total of 403 DEGs being downregulated and 921 DEGs being upregulated (**Fig. 4b**). Gene ontology analysis was conducted on these sets of downregulated and upregulated genes, respectively (**Fig. 4c**, left and right panels, respectively). The set of downregulated genes was characterized by a significant over-representation of genes annotated as being involved in TNF-α or NF-κB signaling and innate immune sensing (**Fig. 4c**, left panel**,** arrows, see **Supplemental Table 5**). Conversely, the set of upregulated genes was characterized by a significant over-representation of genes annotated as being involved in the TGF-β signaling pathway (**Fig. 4c**, right panel, arrow, see **Supplemental Table 6**). This confirmed that pre-exposure to HTLV-1-transformed T cell does influence the transcriptional response to LPS stimulation.

To further identify the expression patterns of these genes differentially expressed between LPS-stimulated C91-PL-pre-exposed MDDCs, and LPS-stimulated Jurkat-pre-exposed MDDCs, we classified these genes based on their differential expression across conditions (detailed in **Supplemental Fig. 7a**, see also **Supplementary Table 4)** as follows: (i) Genes whose responsiveness to LPS (be it repression or induction) is specifically conferred by pre-exposure to infected cells (**Fig. 4d**, upper panel). (ii) Genes whose responsiveness to LPS (be it induction or repression) is exacerbated by pre-exposure to infected cells (**Fig. 4d**, middle panel). (iii) Genes whose responsiveness to LPS is attenuated or (iv) abolished by pre-exposure to infected cells (**Fig. 4d**, lower panel). This classification demonstrates that pre-exposure to HTLV-1-transformed T cells induces both a change in the identity of genes that transcriptionally respond to LPS stimulation, defining a unique LPS-induced transcriptional signature; and a change in the magnitude of the transcriptional response of genes that are normally responsive to LPS.

In line with the gene ontology analysis presented in Fig. 4c, the responsiveness of genes involved in NF-κB signaling, such as *MYD88* (**Fig. 4d**, lower panel, see graph), or the pro-inflammatory genes *CCL2*, *IL12B*, *TNF*, *CXCL10* and *CXCL11* (**Supplementary Fig. 7b**, upper panel), was found drastically attenuated by pre-exposure to infected cells (C91-PL or C8166). This could account for the inefficient maturation and production of pro-inflammatory cytokines by HTLV-1-pre-exposed MDDCs after LPS stimulation, which was observed in Fig. 3. In addition, in line with the gene ontology analysis presented in **Fig. 4c**, genes of the TGF-β signaling pathway, including *BMP6, BMP7,* and *IL13* (**Supplementary Fig. 7b**, middle panel), which do not respond to LPS in normal conditions, were found to be responsive to LPS when MDDCs were pre-exposed to HTLV-1-transformed cells, while the responsiveness of *TGFB2*, which is repressed upon LPS stimulation in normal conditions, was abolished by pre-exposure to HTLV-1-infected cells (**Fig. 4d**, lower panel, see graph).

Interestingly, these genes encode cytokines known to participate in the induction of a tolerogenic immune microenvironment, with Treg and T_H2 responses, which are inefficient at controlling viral infection. Finally, pre-exposure to HTLV-1-transformed cells also conferred responsiveness to *DDIT4* (**Fig. 4d**, upper panel, see graph), a gene reported in other contexts of tolerogenicity[22]. Of note, and in agreement with the efficient induction of IFN-I after LPS stimulation in both Jurkat- or C91-PL-pre-exposed MDDCs (see Fig. 3c), the responsiveness of *ISGs* such as *ISG15, IFI44* and *IRF2* was not affected by pre-exposure to HTLV-1-infected cells (**Supplementary Fig. 7b**, lower panel).

Altogether, this transcriptomic analysis indicated that pre-exposure to HTLV-1-transformed T cells influences the responsiveness of MDDCs to subsequent stimulation, by specifically dampening their pro-inflammatory response at the transcriptional level. In addition, it uncovered the fact that pre-exposure to HTLV-1-transformed T cells allows a unique set of genes to respond to LPS stimulation, triggering a biased, pro-tolerogenic response of MDDCs upon subsequent stimulation.

Neither HTLV-1 viral capture, nor cell-cell contact with infected T cells, are strictly required to dampen the responsiveness of MDDCs to subsequent stimulation

As stated above, RNA-seq analysis using the C8166 infected cell line suggests that viral capture might not be required to alter the transcriptional response of MDDCs to a secondary stimulation. To confirm this notion at the functional level, we repeated the coculture experiment followed by LPS stimulation, and analyzed MDDC maturation profile by flow cytometry (**Fig. 5a**). Despite the lack of viral particle capture by C8166-exposed MDDCs (see **Supplementary Fig. 6**), C8166 pre-exposure still dampened the responsiveness of MDDCs to LPS and R848 stimulation, as monitored through CD86, CD83 or CD80 upregulation, similar to C91-PL pre-exposure (**Fig. 5a and Supplemental Fig. 8a**), confirming that viral capture is

not strictly required. Although C8166 do not produce viral particles, they might still engage in cell-cell contacts with MDDCs[23], which could be the trigger of the dampening of MDDC responsiveness. We addressed this hypothesis by performing the cocultures in transwells, in which MDDCs were physically separated from infected T cells by a permeable membrane (**Fig. 5b**). Of note, reduced but detectable levels of viral capture were detected in MDDCs physically separated from C91-PL (**Supplementary Fig. 8b**), most probably because the virus is preferentially associated to the cell surface of infected cells and might be released as large adhesive viral aggregates[24] poorly able to cross the 0.4µm pores of the permeable membrane. The absence of physical contact between MDDCs and infected T cells, either producing (C91-PL) or not producing viral particles (C8166), did not restore a fully efficient maturation after LPS stimulation (**Fig. 5b**), indicating that cell-cell contacts are not strictly required to allow HTLV-1-infected T cells to manipulate MDDC responsiveness. Of note however, C8166 cells appeared less efficient than C91PL cells in dampening MDDC responsiveness upon transwell coculture. This could result from additive effects of mechanisms dependent on viral capture on the one hand, and of cell-cell contact on the other hand: indeed, in the presence of cell-cell contacts (**Fig. 5a**), the contribution of viral capture might be negligible; while in the absence of cell-cell contacts (**Fig. 5b**), such contribution might become relatively more important. Consistently, comparison of MDDC responsiveness in paired experiments of MDDC pre-exposed to infected cells with (coculture) or without (transwell) physical contacts (**Fig. 5c**) showed that preventing physical contacts between MDDCs and infected cells resulted in a slightly higher, yet not significantly different, MDDC responsiveness (**Fig 5c**). This indicates that viral capture and/or cell-cell contacts may participate, but are not strictly required to allow HTLV-1-infected T cells to manipulate MDDC responsiveness, and suggests the contribution of a distantly acting set of soluble mediators.

A molecular dialogue between HTLV-1-infected T cells and MDDCs induces the release of soluble tolerogenic mediators

Since neither viral particles nor cell-cell contacts are strictly required to manipulate MDDC responsiveness, we then tested the conditioning ability of the supernatant of HTLV-1-infected T cells. More specifically, we hypothesized that IL-10 produced by HTLV-infected T cells[25] could be a candidate mediator, as it was reported to have tolerogenic properties[26]. However, except for the supernatant of the MT-2 infected T cell line, IL-10 was not detected in the supernatant of any of the other infected T cell lines (**Supplementary Fig. 9a**). More surprisingly, none of these supernatants were sufficient to manipulate MDDC responsiveness, as MDDCs pre-incubated in these supernatants still efficiently matured upon LPS stimulation (**Supplementary Fig. 9b**). This suggested that MDDC manipulation requires a molecular dialogue between HTLV-1-transformed T cells and MDDCs that would lead to the production of soluble tolerogenic mediators upon coculture. To test this hypothesis, we collected the conditioned medium of MDDCs cocultured with infected T cells for 24h, and used it to culture fresh, naïve MDDCs derived from the same monocyte donor (autologous cells) for 24h, before LPS stimulation for another 24h (see **Fig. 6a** for the experimental settings). In contrast to supernatant of infected T cells alone (**Supplementary Fig. 9b**), the supernatant from the co-culture was still able to dampen the responsiveness of MDDCs (**Fig. 6b**), although with less potency compared to coculture with infected T cells, as observed by analysis of paired experiments (**Fig. 6c**). This is consistent with the tendency observed upon transwell cultures (see **Fig. 5c**), and confirms the release of soluble tolerogenic mediators following a molecular dialogue between infected T cells and MDDCs upon coculture, which could cooperate with other mechanisms dependent on viral capture and/or cell-cell contacts.

Next, we addressed the kinetics of the molecular dialogue required for the release of these mediators. Conditioned medium of MDDCs cocultured with infected T cells were collected over time, and used to culture fresh autologous MDDCs before the addition of LPS (**Fig. 6d**). A lowered responsiveness of MDDCs was only observed with supernatants collected at least 18h after coculture (**Fig. 6e**), suggesting that the mediators is produced and released after a transcriptional response. Alternatively, we tested the kinetics required for the mediators to manipulate MDDC responsiveness. Conditioned medium of MDDCs cocultured with infected T cells was collected after 24h, and used to culture fresh autologous MDDCs for a varying duration before the addition of LPS (**Fig. 6f**). A lowered responsiveness of MDDCs was only observed when MDDCs were cultured for at least 18h with the conditioned medium before adding the LPS (**Fig. 6g**). The manipulation of MDDC responsiveness might thus also rely on a transcriptional control, which is consistent with the unique transcriptional signature induced by exposure to HTLV-1-infected T cells observed by RNA-seq.

Altogether, our results (recapitulated in **Fig. 6h**) show that upon coculture, a molecular dialogue is initiated between HTLV-1-transformed T cells and MDDCs, which results in the transcriptionally-controlled release of a set of soluble tolerogenic mediators that manipulates MDDC responsiveness, in cooperation with additional mechanisms dependent on viral capture and/or cell-cell contacts.

Discussion

The remarkable ability of viruses to manipulate intracellular pathways in infected host cells is essential for establishing and maintaining infection. In addition to these direct effects, viruses may also establish a specific microenvironment around infected cells, which may favor viral spread and persistence by influencing the signaling pathways and behavior of neighboring, uninfected cells, including immune cells[27,28]. As a by-stander effect, this may alter immune responsiveness to other stimuli. Mechanisms by which viruses influence uninfected cells in their local environment are still poorly understood. In this study, we aimed to decipher how HTLV-1-infected cells indirectly manipulate cocultured DCs. We demonstrate that exposure to HTLV-1-infected T cells induces a unique transcriptional signature in DCs, preventing their maturation and impairing their ability to be subsequently activated. This induction of tolerogenicity is not directly caused by infection of DCs, but instead results from a molecular dialogue between infected T cells and DCs, reminiscent of a viral microenvironment[27,28].

Previous work on the interplay between HTLV-1 and DCs has focused on the role of DCs as intermediate target cells for HTLV-1 transmission to T cells[10–12]. Several studies investigated whether viral capture by DCs could lead to T cell cis- and/or trans-infection, and whether specific DC subtypes or maturation statuses could impact this proviral function. In particular, in a previous paper, we demonstrated that immature MDDCs do efficiently capture and transmit HTLV-1 to T cells, while mature MDDCs do not efficiently transmit HTLV-1 to T cells, despite high levels of viral capture[11]. While these data indicated that the maturation status of DCs could impact their proviral functions, they did not address whether exposure to HTLV-1 induced a antiviral immune response by DCs. Such a question was investigated in pDCs, which we showed to be efficient at sensing HTLV-1-infected cells after cell-cell contact, and at responding by producing IFN-I[20]. Here, we specifically addressed how MDDCs respond to HTLV-1 exposure. Intriguingly, our results are in stark contrast to those

obtained in pDCs, as we show that MDDCs do not respond to HTLV-1-infected T cells by activating a typical maturation and antiviral program, even in the presence of cell-cell contact. The unique transcriptional response observed could be the result of a specific molecular dialogue occurring between HTLV-1-infected T cells and MDDCs, that does not occur with pDCs. Alternatively, this molecular dialogue could also occur with pDCs, but be outperformed by the highly efficient capacity of pDCs to produce IFN-I. Investigating how pDC added to the coculture between HTLV-1-infected T cells and MDDCs could modulate this induction of tolerogenicity, and how this tolerogenic behavior would shape HTLV-1 transmission to uninfected T cells, would give insight into how these distinct behaviors are integrated into the microenvironment system. Of note, our results are also in contrast with data obtained on murine DCs, using cell-free HTLV-1[15]. This underlines the importance of working with human cells when investigating HTLV-1/host interactions.

Our data point towards the release of soluble tolerogenic mediators following a molecular dialogue between infected T cells and MDDCs upon coculture, which could cooperate with other mechanisms dependent on viral capture and/or cell-cell contacts. The identity of the soluble mediators initiating the molecular dialogue observed between HTLV-1-infected T cells and MDDCs, as well as produced as a result of this dialogue, is currently under investigation in our laboratory. As we observed that conditioned medium from infected T cells alone did not induce the tolerogenic behavior of MDDCs, but that conditioned medium from infected T cells cocultured with MDDCs did, it raises the hypothesis that HTLV-1-infected T cells sense a soluble factor released by MDDCs, that activates the release of a second soluble factor by infected T cells. This second factor could then launch a specific transcriptomic response in MDDCs that would lead to tolerogenicity. Among potential soluble mediators produced by HTLV-1-infected cells, exosomes emerge as compelling candidates. Their composition could be modified by viral infection, explaining the differences

observed in MDDC responses between exposure to uninfected or infected T cells. Also, their production by T cells could be boosted by coculture with MDDCs, explaining the requirement of a molecular dialogue between both cell types. Last, the diameter of exosomes, around 100 nm, is compatible with their diffusion through the pores of the transwell (0.4 µm) used in our experimental settings. Interestingly, several HTLV-1-infected T cell lines, independently of their ability to produce viral particles or not, do produce exosomes containing cytokines, viral proteins and RNA[29–31] able to modulate target cells, resulting in an increased susceptibility to infection[23]. We can thus hypothesize that in our experimental settings, these exosomes could modulate DC functions, inducing the unique transcriptional signature that we observe. This would be reminiscent of data obtained on Epstein-Barr Virus (EBV), where infection changes the ability of exosomes purified from gastric cancer cell lines to mature MDDCs, leading to a defect in CD86 upregulation and reduced tumor immunity[32].

Whether HTLV-1 proteins contained in exosomes could contribute to the induction of tolerogenicity remains to be investigated. Viral proteins such as p30, HBZ, and Tax are found in exosomes produced by infected cells[23,29], independently of the production of viral particles by these infected cells. In addition, these viral proteins have the potential to interfere with immune functions. For instance, p30 expressed in MDDCs reduces IFN-I responses upon TLR3/4 stimulation, but not upon TLR7/8 stimulation[33], suggesting a specific targeting of the TLR3/4 signaling pathway. However, as we found no alteration in the IFN response of LPS restimulated, HTLV-1-pre-exposed MDDCs, a role of p30 can be excluded. In contrast, HBZ is known to inhibit the NF-κB pathway[34] by degrading the transcription factor p65[35]. As we observed the repression of the NF-κB pathway in HTLV-1-pre-exposed MDDCs upon LPS restimulation, we could suggest that exosome-transferred HBZ could contribute to modulating MDDC functions.

Interestingly, following the molecular dialogue between infected T cells and MDDCs, we observed the upregulation of genes involved in fatty acid metabolism (such as *ELOVL3*, *FADS1*, and *SLC27A6*) in MDDCs. As these genes are not found in the typical maturation program of MDDCs, it raises the possibility that upon coculture with HTLV-1-infected T cells, MDDCs produce fatty acids, that may act in a autocrine and paracrine manner to modulate MDDC functions. Of note, fatty acid precursors such as squalene and vitamin D are recognized inducers of tolerogenic DCs[36,37]. Polyinsaturated fatty acids have also been shown to block DC activation and functions[38], and inhibition of fatty acid synthesis has been shown to increase their production of pro-inflammatory cytokines[39]. Whether HTLV-1-exposed MDDCs produce higher levels of fatty acids, and whether these could contribute to their observed tolerogenic behavior, is currently under investigation. Thus, our transcriptomic analysis reveals how viruses could indirectly rewire lipid metabolism in immune cells to modulate the immune microenvironment.

Upon restimulation with LPS, HTLV-1-pre-exposed MDDCs undergo a specific transcriptomic response, including an abolished downregulation of *TGFB* expression, which remains highly expressed, and upregulation of *IL13* expression, which could be the basis for their tolerogenic properties. Of note, from the literature, the exact transcriptomic program underlying the tolerogenic behavior of DCs is unclear, as different transcriptomic signatures have been reported[40–42]. Nonetheless, a set of common genes has been defined as a gene signature of tolerogenic DCs[22], including *DDIT4* (DNA-damage-inducible transcript 4), which encodes an inhibitor of mTOR signaling[22]. Interestingly, responsiveness of *DDIT4* was also specifically conferred by pre-exposure to infected cells. Thus, the transcriptomic program induced in HTLV-1-pre-exposed MDDCs by LPS restimulation partially mirrors the tolerogenic DC signature defined in other contexts.

In conclusion, our study demonstrates that exposure to HTLV-1-transformed cells can indirectly distort the functionality of DCs and impair their response to subsequent stimulation. Our *in vitro* results are consistent with *in vivo* observations, which report that MDDCs from HTLV-1-infected patients exhibit deficiencies in both basal maturation and responsiveness to TNF-α treatment, as well as defects in the induction of T-cell response[16,17]. In addition, PBMCs from HTLV-1-infected patients stimulated with tuberculin produce fewer TNF-α than PBMC isolated from healthy individuals[43]. Finally, the fact that viral production is not necessary to dampen MDDC responsiveness, might reflect the *in vivo* situation in which HTLV-1 expression is repressed in chronically infected cells[44]. Therefore, it is plausible that defects in the myeloid cell response, particularly in DCs, may represent a mechanism of HTLV-1 pathogenesis *in vivo*. Thus, this work illustrates how HTLV-1 might induce a local immune microenvironment suitable for its own persistence. Such microenvironnement may additionally contribute to by-stander immune dysfunctions, in asymptomatic HTLV-1 carriers as well as symptomatic HTLV-1-infected patients.

Methods

Cells lines

HTLV-1 infected T-cell lines (C91-PL from Cellosaurus ref CVCL_0197, MT-2 ref CVCL_2631[45], Hut102 ref CVCL_3526[46] and C8166 ref ECACC 88051601[21]) and control uninfected T-cell lines (Jurkat from ATCC ref ACC 282, CEM/C1 ref CRL-2265, Molt-4 Cellosaurus ref CVCL_0013) were maintained at a cell density of $0.5.10^6$ cells/mL in complete RPMI medium: RPMI1640 GlutaMAX (Gibco; 61870010) supplemented with 10% fetal calf serum (FCS) and penicillin-streptomycin (100 U/mL and 100 µg/mL respectively).

The human fibrosarcoma cell line HL116 stably expressing the firefly luciferase reporter gene under the control of the immediate early IFN-I inducible 6-16 promoter (kindly provided by Dr. S. Pelligrini, Institut Pasteur, France[47]) was maintained under HAT selection (Gibco; 21060017, used at 1X final concentration) in DMEM GlutaMAX pyruvate medium (Gibco; 10569010) supplemented with 10% FCS and penicillin-streptomycin (100 U/mL and 100 µg/mL respectively).

All cells were grown at 37°C in 5% CO_2 and tested negative for mycoplasma contamination on a regular basis. None of the cell lines were authenticated.

Human primary monocyte-derived dendritic cells (MDDCs)

MDDCs were derived from purified monocytes from healthy blood donors as described previously[11]. Briefly, blood samples were collected at Etablissement Français du Sang (EFS) from anonymous healthy blood donors according to the institutional Standard Operating Procedures for blood donation, including a signed informed consent. Blood was diluted in PBS 1X (Gibco) and peripheral blood mononuclear PBMCs were isolated using a density gradient separation using Ficoll-Paque (Fisher Scientific, 11778538). Monocytes were then isolated from PBMCs using a density gradient separation using Percoll Centrifugation Medium

(Fisher Scientific, 10607095). Freshly or frozen monocytes were cultured in six-well plates at 3.10^6 cells/mL in complete MDDC medium: RPMI1640 GlutaMAX (Gibco) supplemented with 10% FCS, penicillin-streptomycin (100 U/mL and 100 µg/mL respectively), Hepes buffer (Gibco, 15630080; 10 mM), MEM non-essential amino acids (2,5mM, Gibco, 11140050), sodium pyruvate (Gibco, 11360070; 1 mM), and beta-mercaptoethanol (Gibco, 31350-010; 0.05 mM). MDDC medium was supplemented with IL-4 and GM-CSF (Miltenyi Biotec, 130-093-922 and 130-093-866; 100 ng/mL each) for differentiation. On day 3, the culture medium was refreshed by discarding half of the medium and adding the same volume of new MDDC medium and twice concentrated IL-4 and GM-CSF to all cell cultures. Immature MDDCs were harvested on day 5 or 6. Every experiment was repeated on MDDCs derived from independent blood donors.

Reagents and antibodies

Toll-like receptor (TLR)-4 agonist (LPS, tlrl-3pelps; 1µg/mL) and TLR-7/8 agonist (R848, tlrl-r848; 3µg/mL) were purchased from Invivogen. MeV IC323-eGFP [48] is a recombinant MeV expressing the gene-encoding eGFP (using the plasmid-encoding MeV IC323-eGFP kindly provided by Yanagi, Kyushu University, Fukuoka, Japan). MeV IC323 recombinant virus was rescued in 293-3-46 cells, as previously described[49]. Production of the viruses was performed at 32°C. All viruses were propagated and titrated in Vero-SLAM/CD150 cells. MDDCs were infected using a multiplicity of infection (MOI) of 1.

The following antibodies were used: V450-coupled mouse anti-Human CD11c (BD Biosciences, 560369; 1/100), PE-coupled mouse anti-Human CD86 (Invitrogen, 12-0869-42; 1/100), APC-coupled mouse anti-Human CD83 (Miltenyi Biotec, 130-094-186; 1/50), BV510-coupled mouse anti-Human CD83 (BD Biosciences, 563223; 1/50), APC-H7-coupled mouse anti-Human CD80 (BD Biosciences, 561134; 1/50), BB515-coupled mouse anti-

Human PD-L1 (BD Biosciences, 564554; 1/25), PE-Cy7-coupled mouse anti-Human ICOSL (BioLegend, 309410; 1/100), Mouse anti-Gagp19 clone TP7 (Zeptometrix, 081107; 1/500), AlexaFluor647-coupled Alpaca anti-Mouse IgG1 (Chromotek, sms1AF647-1-5; 1/500), Biotin-coupled mouse anti-Human CADM1 (MBL Life Sciences, CM004-6; 1/1000), AlexaFluor647-coupled mouse streptavidin (Invitrogen, S31374; 1/500).

MDDCs coculture experiment

Immature MDDCs (3.10^5 cells) were plated in 48-well plates and cocultured with HTLV-1-infected or control uninfected T-cells (6.10^4 cells) in 300µL complete MDDC medium supplemented with IL-4 and GM-CSF for 24h or 48h. When indicated, transwell 24-well plates with permeable polycarbonate membrane inserts (0.4µm diameter) were used (Fisher Scientific, 10147291). Alternatively, MDDCs were cultured in supernatant collected from either HTLV-1-infected or control uninfected T-cell culture, or from coculture of MDDCs with HTLV-1-infected cells or control uninfected T-cell during 24h (or the indicated duration). After 24h, cells were harvested, or stimulated with LPS or R848 or medium for an additional 24h (or the indicated duration). At the indicated time points, cells and supernatants were collected for phenotyping using flow cytometry and for cytokine quantification, respectively.

Flow cytometry analysis

To assess surface marker expression, cells were fixed using 4% paraformaldehyde (PFA) diluted from 20% PFA (Electron Microscopy Science, 50-980-493) in PBS 1X, and stained with the indicated surface markers antibodies diluted in PBS 1X-1% Bovine Serum Albumin (BSA) for 20 min at 4°C. To assess viral capture, cells were fixed and permeabilized using the Fix/Perm FoxP3 and Transcription factors kit (Invitrogen, 00-5523-00) according to the

manufacturer's instructions, and stained with mouse anti-Gagp19 antibody followed by the AlexaFluor647-coupled anti-mouse antibody diluted in the PERM buffer supplemented with 7% Normal Goat Serum (NGS) for 25 min at room temperature. Cells were then stained for the indicated surface markers diluted in PBS 1X 1% BSA as described above. Compensation beads (BD Biosciences, 552843) were used to correct signal overlap between the emission spectra of the different fluorophores.

Data were acquired using a flow cytometer FACS CantoII (BD Biosciences) and analyzed with FlowJo v10.7 software (BD Life Sciences). The full gating strategy is exemplified in **Supplementary Fig. 1**.

Cytokine quantification

TNF-α and IL-10 were quantified in the collected supernatants using Bio-Plex Pro Human Luminex kit (Bio-Rad) according to the manufacturer's instructions.

Type I interferon quantification

HL116 cells were seeded at 2.10^4 cells/well in 96-U-bottom-well plates and incubated for 24h. Supernatant collected from MDDCs culture (100 µL) or serial dilutions of recombinant IFN-α (Tebu-Bio, RPA033Gu02) used for standard curve determination were added for an additional 17h. Cells were then lysed (Promega Passive Lysis Buffer, E1941) and luciferase activity assayed according to the manufacturer's instruction (Promega Luciferase Assay System, E1501).

MDDCs isolation after coculture

Cells from MDDC / T-cell lines coculture (1.10^6 MDDCs and 2.10^5 T-cells) were harvested and stained using biotin-coupled anti-CADM1 followed by AlexaFluor647-coupled streptavidin diluted in PBS 1X-1% BSA for 20 min at 4°C. After several washes in PBS, cells

were then incubated with anti-AlexaFluor647 MicroBeads (Miltenyi Biotec, 130-091-395) and separated on MACS Separation LD Columns (Miltenyi Biotec, 130-042-901) according to the manufacturer's instructions. To assess the purity and yield of enrichment of MDDCs after magnetic separation, 6.10^4 cells were collected before and after separation on LD columns, fixed in 4% PFA and stained with CD11c-V450 antibody, before analysis using FACS Canto II.

RNA preparation

After magnetic separation, MDDCs were lysed and total RNA was extracted using the NucleoSpin RNA Mini kit for RNA purification (Macherey-Nagel, 740955) according to the manufacturer's instructions. RNA concentration was determined with a NanoDropND1000 spectrophotometer (Thermo Fisher Scientific) and samples were stored at -80°C until shipment for external sequencing. Stranded RNA libraries were prepared after removal of rRNA. High throughput sequencing of 150 bp paired-end reads was performed with an Illumina HiSeq 2500 platform by Novogene Europe (Cambridge, United Kingdom). Each sample had on average 50 million matched pairs of reads.

RNA-seq data analysis

The quality of sequences was checked using the FastQC tool. The reads were trimmed with PrinSeq[50] to remove low-quality bases and then mapped to the human reference transcriptome (hg19) using Kallisto pseudoalignment[51]. Differential gene analysis was carried out with DESeq2 package[52]. Genes with a basemean >10 showing an absolute fold change (FC) $\geq$ 2 with an adjusted p-value <0.05 (Wald test using Benjamini and Hochberg method) were considered differentially expressed. All DEGs identified in this study are listed in Supplementary Table 1 and 4. DAVID functional annotation tool using the KEGG pathways database was used for gene ontology analysis[53,54]. For clarity, KEGG pathways were filtered and grouped as listed in Supplementary Table 2 to reduce redundancy.

To identify the expression pattern responsiveness in LPS-stimulated MDDC pre-exposed to C91-PL, we retrieved the genes by Venn analysis using the following list of DEGs: MDDC/Jurkat restim.w/LPS vs MDDC/Jurkat; MDDC/C91-PL restim.w/LPS vs MDDC/Jurkat restim.w/LPS; MDDC/C91-PL restim.w/LPS vs MDDC/Jurkat. Then, genes were classified as follows (summarized in **Supplementary Fig 7a**): (i) responsiveness confered by pre-exposure to infected cells: genes that are not differentially expressed between mock- and LPS-stimulated Jurkat-pre-exposed MDDCs, but are differentially expressed (either up or down) between mock-stimulated Jurkat-pre-exposed MDDCs and LPS-stimulated C91-PL-pre-exposed MDDCs; (ii) responsiveness exacerbated by pre-exposure to infected cells: genes that are either up-regulated in LPS-stimulated Jurkat-pre-exposed MDDCs, compared to mock-stimulated Jurkat-pre-exposed MDDCs, and further up-regulated in LPS-stimulated C91-PL-pre-exposed MDDCs, compared to LPS-stimulated Jurkat-pre-exposed MDDCs; or down-regulated in LPS-stimulated Jurkat-pre-exposed MDDCs compared, to mock-stimulated Jurkat-pre-exposed MDDCs, and further down-regulated in LPS-stimulated C91-PL-pre-exposed MDDCs, compared to LPS-stimulated Jurkat-pre-exposed MDDCs; (iii) responsiveness attenuated by pre-exposure to infected cells: genes that are either up-regulated in LPS-stimulated Jurkat-pre-exposed MDDCs, compared to mock-stimulated Jurkat-pre-exposed MDDCs, as well as up-regulated in LPS-stimulated C91-PL-pre-exposed MDDCs, compared to mock-stimulated Jurkat-pre-exposed MDDCs, but down-regulated in LPS-stimulated C91-PL-pre-exposed MDDCs, compared to LPS-stimulated Jurkat-pre-exposed MDDCs; or down-regulated in LPS-stimulated Jurkat-pre-exposed MDDCs, compared to mock-stimulated Jurkat-pre-exposed MDDCs, in LPS-stimulated C91-PL-pre-exposed MDDCs, compared to mock-stimulated Jurkat-pre-exposed MDDCs, but up-regulated in LPS-stimulated C91-PL-pre-exposed MDDCs, compared to LPS-stimulated Jurkat-pre-exposed MDDCs; (iv) responsiveness abolished by pre-exposure to infected cells:

genes that are either up-regulated in LPS-stimulated Jurkat-pre-exposed MDDCs, compared to mock-stimulated Jurkat-pre-exposed MDDCs, as well as down-regulated in LPS-stimulated C91-PL-pre-exposed MDDCs, compared to LPS-stimulated Jurkat-pre-exposed MDDCs, but not differentially expressed in LPS-stimulated C91-PL-pre-exposed MDDCs, compared to mock-stimulated Jurkat-pre-exposed MDDCs; or down-regulated in LPS-stimulated Jurkat-pre-exposed MDDCs compared to mock-stimulated Jurkat-pre-exposed MDDCs, as well as up-regulated in LPS-stimulated C91-PL-pre-exposed MDDCs, compared to LPS-stimulated Jurkat-pre-exposed MDDCs, but not differentially expressed in LPS-stimulated C91-PL-pre-exposed MDDCs, compared to mock-stimulated Jurkat-pre-exposed MDDCs.

Statistical analysis

Median fluorescence intensity and percentages of gated cells were determined from flow cytometry analysis with FlowJo software. Data were analyzed using Prism 8 (GraphPad Software). The central tendency represents the mean, and the error bar represents the standard error of the mean (SEM).Statistical analysis was performed as follows: normality of the dataset was tested using Shapiro Wilk test. If the dataset followed a Gaussian distribution, differences among means were tested using Repeated measures one-way ANOVA, or Ordinary one-way ANOVA when the dataset contained missing values. Post-hoc comparisons with the mean of the control condition (exposure to uninfected Jurkat T cells) were assessed with Dunnet's test. Note that for Figure 1e, Sidak's test was used to compare the means of the C91-PL-exposed MDDCs depending on their capture status.

When normality of the dataset was not met, analysis was performed using Friedman test, or Kruskal Wallis test when the dataset had missing values. Post-hoc comparisons with the mean of the control condition (exposure to uninfected Jurkat T cells) were performed using Dunn's test.

For main Figures that are subsets of larger supplementary figures, the indicated p-values are reported from the analysis on the total dataset.

When only two groups were compared, statistical analysis was performed using parametric paired t-test (Figures 5c and 6c, Sup Figure 8b) or its non-parametric equivalent Wilcoxon matched-pairs signed rank test (Figure 5c). Note that a parametric unpaired Welch's t-test was used to analyze Figure 6g due to the uneven number of replicates.

The potential correlation investigated in Supplementary Figure 2i was fitted with a simple linear regression model. p-value < 0.05 was considered significant, and statistics are denoted as * $p<0.05$, ** $p<0.01$, *** $p<0.001$, **** $p<0.0001$.

Data Availability

The RNA-seq raw data generated in the present study were deposited in GEO under the accession number GSE266976.

References

1. Bangham, C. R. M. Human T Cell Leukemia Virus Type 1: Persistence and Pathogenesis. *Annu. Rev. Immunol.* **36**, 43–71 (2018).
2. Gordon, C. A. *et al.* HTLV-I and Strongyloides in Australia: The worm lurking beneath. *Adv. Parasitol.* **111**, 119–201 (2021).
3. Haziot, M. E. *et al.* Detection of clinical and neurological signs in apparently asymptomatic HTLV-1 infected carriers: Association with high proviral load. *PLoS Negl. Trop. Dis.* **13**, e0006967 (2019).
4. Kagdi, H., Demontis, M. A., Ramos, J. C. & Taylor, G. P. Switching and loss of cellular cytokine producing capacity characterize in vivo viral infection and malignant transformation in human T- lymphotropic virus type 1 infection. *PLoS Pathog.* **14**, e1006861 (2018).
5. Paquin-Proulx, D. *et al.* MAIT cells are reduced in frequency and functionally impaired in human T lymphotropic virus type 1 infection: Potential clinical implications. *PloS One* **12**, e0175345 (2017).
6. de Castro-Amarante, M. F. *et al.* Human T Cell Leukemia Virus Type 1 Infection of the Three Monocyte Subsets Contributes to Viral Burden in Humans. *J. Virol.* **90**, 2195–2207 (2015).
7. Kannagi, M., Hasegawa, A., Takamori, A., Kinpara, S. & Utsunomiya, A. The roles of

acquired and innate immunity in human T-cell leukemia virus type 1-mediated diseases. *Front. Microbiol.* **3**, 323 (2012).
8. Dalod, M., Chelbi, R., Malissen, B. & Lawrence, T. Dendritic cell maturation: functional specialization through signaling specificity and transcriptional programming. *EMBO J.* **33**, 1104–1116 (2014).
9. Rescigno, M. Dendritic cell functions: Learning from microbial evasion strategies. *Semin. Immunol.* **27**, 119–124 (2015).
10. Jones, K. S., Petrow-Sadowski, C., Huang, Y. K., Bertolette, D. C. & Ruscetti, F. W. Cell-free HTLV-1 infects dendritic cells leading to transmission and transformation of CD4(+) T cells. *Nat. Med.* **14**, 429–436 (2008).
11. Rizkallah, G. *et al.* Dendritic cell maturation, but not type I interferon exposure, restricts infection by HTLV-1, and viral transmission to T-cells. *PLoS Pathog.* **13**, e1006353 (2017).
12. Alais, S., Mahieux, R. & Dutartre, H. Viral Source-Independent High Susceptibility of Dendritic Cells to Human T-Cell Leukemia Virus Type 1 Infection Compared to That of T Lymphocytes. *J. Virol.* **89**, 10580–10590 (2015).
13. Valeri, V. W. *et al.* Requirement of the human T-cell leukemia virus p12 and p30 products for infectivity of human dendritic cells and macaques but not rabbits. *Blood* **116**, 3809–3817 (2010).
14. Galli, V. *et al.* Essential Role of Human T Cell Leukemia Virus Type 1 orf-I in Lethal Proliferation of CD4+ Cells in Humanized Mice. *J. Virol.* **93**, e00565-19 (2019).
15. Rahman, S. *et al.* Murine FLT3 ligand-derived dendritic cell-mediated early immune responses are critical to controlling cell-free human T cell leukemia virus type 1 infection. *J. Immunol. Baltim. Md 1950* **186**, 390–402 (2011).
16. Nascimento, C. R. *et al.* Monocytes from HTLV-1-infected patients are unable to fully mature into dendritic cells. *Blood* **117**, 489–499 (2011).
17. Makino, M., Wakamatsu, S., Shimokubo, S., Arima, N. & Baba, M. Production of functionally deficient dendritic cells from HTLV-I-infected monocytes: implications for the dendritic cell defect in adult T cell leukemia. *Virology* **274**, 140–148 (2000).
18. Makino, M., Shimokubo, S., Wakamatsu, S. I., Izumo, S. & Baba, M. The role of human T-lymphotropic virus type 1 (HTLV-1)-infected dendritic cells in the development of HTLV-1-associated myelopathy/tropical spastic paraparesis. *J. Virol.* **73**, 4575–4581 (1999).
19. Azakami, K. *et al.* Severe loss of invariant NKT cells exhibiting anti-HTLV-1 activity in patients with HTLV-1-associated disorders. *Blood* **114**, 3208–3215 (2009).
20. Assil, S. *et al.* Sensing of cell-associated HTLV by plasmacytoid dendritic cells is regulated by dense β-galactoside glycosylation. *PLoS Pathog.* **15**, e1007589 (2019).
21. Bhat, N. K., Adachi, Y., Samuel, K. P. & Derse, D. HTLV-1 gene expression by defective proviruses in an infected T-cell line. *Virology* **196**, 15–24 (1993).
22. Avancini, D. *et al.* Aryl hydrocarbon receptor activity downstream of IL-10 signaling is required to promote regulatory functions in human dendritic cells. *Cell Rep.* **42**, 112193 (2023).
23. Pinto, D. O. *et al.* Extracellular vesicles from HTLV-1 infected cells modulate target cells and viral spread. *Retrovirology* **18**, 6 (2021).
24. Pais-Correia, A.-M. *et al.* Biofilm-like extracellular viral assemblies mediate HTLV-1 cell-to-cell transmission at virological synapses. *Nat. Med.* **16**, 83–89 (2010).
25. Mori, N. *et al.* Interleukin-10 gene expression in adult T-cell leukemia. *Blood* **88**, 1035–1045 (1996).
26. Scheib, N. *et al.* The Dendritic Cell Dilemma in the Skin: Between Tolerance and Immunity. *Front. Immunol.* **13**, 929000 (2022).
27. Song, B. *et al.* Intercellular communication within the virus microenvironment affects

the susceptibility of cells to secondary viral infections. *Sci. Adv.* **9**, eadg3433 (2023).
28. Yogev, O. *et al.* Herpesviruses shape tumour microenvironment through exosomal transfer of viral microRNAs. *PLOS Pathog.* **13**, e1006524 (2017).
29. Pinto, D. O. *et al.* HTLV-1 Extracellular Vesicles Promote Cell-to-Cell Contact. *Front. Microbiol.* **10**, 2147 (2019).
30. Jaworski, E. *et al.* Human T-lymphotropic Virus Type 1-infected Cells Secrete Exosomes That Contain Tax Protein. *J. Biol. Chem.* **289**, 22284–22305 (2014).
31. Kim, Y. *et al.* Extracellular Vesicles from Infected Cells Are Released Prior to Virion Release. *Cells* **10**, 781 (2021).
32. Hinata, M. *et al.* Exosomes of Epstein-Barr Virus-Associated Gastric Carcinoma Suppress Dendritic Cell Maturation. *Microorganisms* **8**, 1776 (2020).
33. Fenizia, C. *et al.* Human T-cell leukemia/lymphoma virus type 1 p30, but not p12/p8, counteracts toll-like receptor 3 (TLR3) and TLR4 signaling in human monocytes and dendritic cells. *J. Virol.* **88**, 393–402 (2014).
34. Huang, J., Ren, T., Guan, H., Jiang, Y. & Cheng, H. HTLV-1 Tax Is a Critical Lipid Raft Modulator That Hijacks IκB Kinases to the Microdomains for Persistent Activation of NF-κB *. *J. Biol. Chem.* **284**, 6208–6217 (2009).
35. Zhao, T. *et al.* Human T-cell leukemia virus type 1 bZIP factor selectively suppresses the classical pathway of NF-κB. *Blood* **113**, 2755–2764 (2009).
36. van Megen, K. M. *et al.* 1,25-dihydroxyvitamin D3 induces stable and reproducible therapeutic tolerogenic dendritic cells with specific epigenetic modifications. *Cytotherapy* **23**, 242–255 (2021).
37. Navarro-Barriuso, J. *et al.* Vitamin D3-Induced Tolerogenic Dendritic Cells Modulate the Transcriptomic Profile of T CD4+ Cells Towards a Functional Hyporesponsiveness. *Front. Immunol.* **11**, 599623 (2020).
38. Zeyda, M. *et al.* Polyunsaturated Fatty Acids Block Dendritic Cell Activation and Function Independently of NF-κB Activation *. *J. Biol. Chem.* **280**, 14293–14301 (2005).
39. Rehman, A. *et al.* Role of Fatty-acid Synthesis in Dendritic Cell Generation and Function. *J. Immunol. Baltim. Md 1950* **190**, 4640–4649 (2013).
40. Robertson, H. *et al.* Transcriptomic Analysis Identifies A Tolerogenic Dendritic Cell Signature. *Front. Immunol.* **12**, 733231 (2021).
41. Navarro-Barriuso, J. *et al.* Comparative transcriptomic profile of tolerogenic dendritic cells differentiated with vitamin D3, dexamethasone and rapamycin. *Sci. Rep.* **8**, 14985 (2018).
42. Schinnerling, K., García-González, P. & Aguillón, J. C. Gene Expression Profiling of Human Monocyte-derived Dendritic Cells – Searching for Molecular Regulators of Tolerogenicity. *Front. Immunol.* **6**, 528 (2015).
43. Carvalho, N. B. *et al.* Impaired TNF, IL-1β, and IL-17 production and increased susceptibility to Mycobacterium tuberculosis infection in HTLV-1 infected individuals. *Tuberculosis* **108**, 35–40 (2018).
44. Kinpara, S. *et al.* Stromal cell-mediated suppression of human T-cell leukemia virus type 1 expression in vitro and in vivo by type I interferon. *J Virol* **83**, 5101–8 (2009).
45. Morozov, V. A. & Weiss, R. A. Two types of HTLV-1 particles are released from MT-2 cells. *Virology* **255**, 279–284 (1999).
46. Bunn, P. A. & Foss, F. M. T-cell lymphoma cell lines (HUT102 and HUT78) established at the National Cancer Institute: history and importance to understanding the biology, clinical features, and therapy of cutaneous T-cell lymphomas (CTCL) and adult T-cell leukemia-lymphomas (ATLL). *J. Cell. Biochem. Suppl.* **24**, 12–23 (1996).
47. Uzé, G. *et al.* Domains of interaction between alpha interferon and its receptor components. *J. Mol. Biol.* **243**, 245–257 (1994).

48. Ferren, M. *et al*. Early Permissiveness of Central Nervous System Cells to Measles Virus Infection Is Determined by Hyperfusogenicity and Interferon Pressure. *Viruses* **15**, 229 (2023).
49. Radecke, F. *et al.* Rescue of measles viruses from cloned DNA. *EMBO J.* **14**, 5773–5784 (1995).
50. Schmieder, R. & Edwards, R. Quality control and preprocessing of metagenomic datasets. *Bioinforma. Oxf. Engl.* **27**, 863–864 (2011).
51. Bray, N. L., Pimentel, H., Melsted, P. & Pachter, L. Near-optimal probabilistic RNA-seq quantification. *Nat. Biotechnol.* **34**, 525–527 (2016).
52. Love, M. I., Huber, W. & Anders, S. Moderated estimation of fold change and dispersion for RNA-seq data with DESeq2. *Genome Biol.* **15**, 550 (2014).
53. Huang, D. W., Sherman, B. T. & Lempicki, R. A. Systematic and integrative analysis of large gene lists using DAVID bioinformatics resources. *Nat. Protoc.* **4**, 44–57 (2009).
54. Sherman, B. T. *et al.* DAVID: a web server for functional enrichment analysis and functional annotation of gene lists (2021 update). *Nucleic Acids Res.* **50**, W216-221 (2022).

Acknowledgements

We dedicate this work to the memory of Pr. Renaud Mahieux. We thank the Retroviral Oncogenesis team, as well as Dr. Arnaud Moris, Dr. Sylvain Baize, Dr. Anne-Sophie Beignon, Pr. Luc Willems, Dr. Franck Halary, Dr. Claudine Pique, Pr. Mathias Faure and Dr. Delphine Muriaux for helpful discussion and/or critical reading of the manuscript. This work has benefited from the facilities and expertise of the SFR Biosciences Lyon (UMS3444/CNRS, US8/Inserm, ENS de Lyon, UCBL). We acknowledge the contribution of the Etablissement Français du Sang Auvergne - Rhône-Alpes, and we thank Dr. Marlène Dreux (CIRI) and her team for the help with PBMC isolation. We thank Dr. Carine Rey (BIBS, CIRI, Lyon) for her help with RNA-seq data analysis. This work was supported by the "Fondation pour la Recherche Médicale, équipe labellisée" program (grant number DEQ. 20180339200), and by the "Agence Nationale de la Recherche" (grant number ANR-22-CE15-0044). AC and CJ are funded by the ENS de Lyon. FM, SA, and HD are funded by Inserm. CM is funded by CNRS.

Author Contributions

Conception and design of the work: HD. Acquisition, analysis, or interpretation of data: AC, FM, SA, CM, CJ, HD. Initial draft of the manuscript: AC, HD. Revision of the manuscript: HD, CM, FM and CJ. Approval of manuscript: AC, SA, CM, FM, CJ and HD.

Competing Interests statement

The authors declare no competing interests.

865

Figure 1

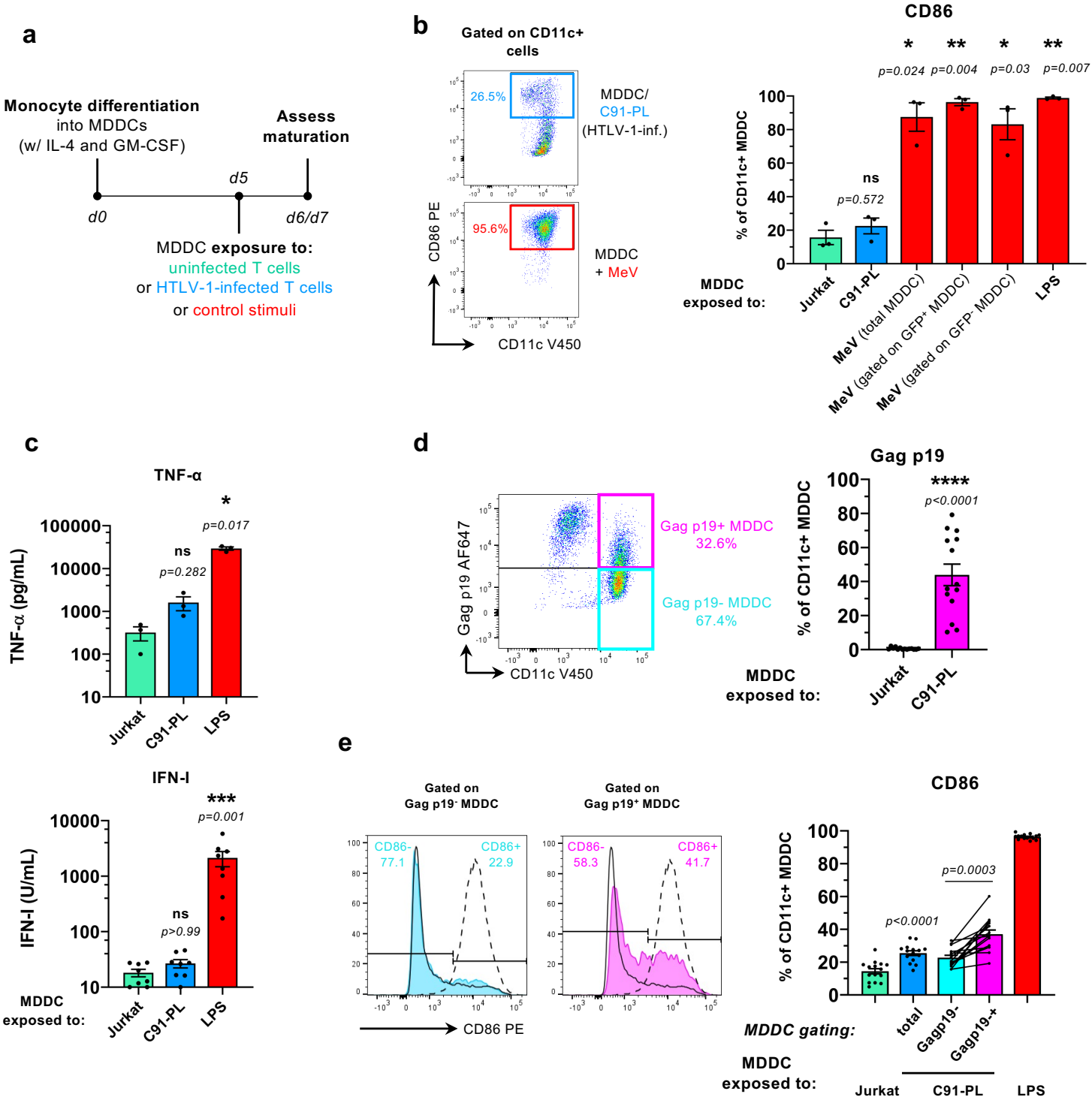
a
Monocyte differentiation
into MDDCs
(w/ IL-4 and GM-CSF)
Assess
maturation
d0
d5
d6/d7
MDDC exposure to:
uninfected T cells
or HTLV-1-infected T cells
or control stimuli
b
Gated on CD11c+
cells
26.5%
MDDC/
C91-PL
(HTLV-1-inf.)
95.6%
MDDC
+ MeV
CD86 PE
CD11c V450
CD86
% of CD11c+ MDDC
ns
p=0.572
p=0.024
p=0.004
p=0.03
p=0.007
MDDC
exposed to:
Jurkat
C91-PL
MeV (total MDDC)
MeV (gated on GFP+ MDDC)
MeV (gated on GFP- MDDC)
LPS
c
TNF-α
TNF-α (pg/mL)
ns
p=0.282
p=0.017
Jurkat
C91-PL
LPS
IFN-I
IFN-I (U/mL)
ns
p>0.99
p=0.001
MDDC
exposed to:
Jurkat
C91-PL
LPS
d
Gag p19 AF647
CD11c V450
Gag p19+ MDDC
32.6%
Gag p19- MDDC
67.4%
Gag p19
% of CD11c+ MDDC
p<0.0001
MDDC
exposed to:
Jurkat
C91-PL
e
Gated on
Gag p19- MDDC
Gated on
Gag p19+ MDDC
CD86-
77.1
CD86+
22.9
CD86-
58.3
CD86+
41.7
CD86 PE
CD86
% of CD11c+ MDDC
p<0.0001
p=0.0003
MDDC gating:
total
Gagp19-
Gagp19-+
MDDC
exposed to:
Jurkat
C91-PL
LPS
f
HTLV-1
infected cells
Immature
MDDCs
24h exposure
Poorly matured
MDDCs
maturation
markers
+/-
IFN-I
+/-
TNF-α
+/-
LPS
Immature
MDDCs
24h exposure
Fully matured
MDDCs
maturation
markers
+++
IFN-I
+++
TNF-α
+++

Figure 1. Human MDDCs do not fully mature when exposed to HTLV-1-infected T cells. a. Schematic representation of the experimental setting. From day 0 (d0), monocytes were differentiated into MDDCs by a 5-day culture in the presence of IL-4 and GM-CSF. At day 5 (d5), MDDCs were cocultured with control uninfected or HTLV-1-infected T cell lines for 24h (or 48h, see Supplementary Fig. 2a-f). Alternatively, MDDCs were stimulated with GFP-expressing MeV or LPS (control stimuli) for 24h (or 48h, see Supplementary Fig. 2a-f). Cells and culture supernatants were collected at d6 (or d7, see Supplementary Fig. 2a-f). **b.** Flow cytometry analysis at d6 after CD11c and CD86 staining. The percentage of $CD86^+$ MDDCs (indicated gate) among total $CD11c^+$ MDDCs was quantified. **Left**: representative experiment. **Right**: results from n=3 independent experiments, analyzed with RM one-way ANOVA as described in Supplementary Table 7. **c.** Supernatant from the indicated cocultures or from LPS-stimulated MDDCs was collected at d6, and TNF-α (**top**) and IFN-I (**bottom**) were quantified by Luminex and reporter cell assay, respectively. Results from n=3 or 8 independent experiments, respectively. Presented data are a subset of Supplementary Figure 2g analyzed with RM one-way ANOVA (top) or Kruskal-Wallis test (bottom) as described in Supplementary Table 7&8. **d.** Viral capture in MDDCs cocultured with Jurkat or C91-PL T cells was assessed at d6 by Gag p19 staining on $CD11c^+$ MDDCs. The percentage of Gag $p19^+$ and Gag $p19^-$ MDDCs among total $CD11c^+$ MDDCs was determined. **Left**: representative experiment. **Right**: results from n=14 independent experiments analyzed with Kruskal-Wallis test as described in Supplementary Table 7&8 as a subset of Supplementary Figure 2h. **e.** Flow cytometry analysis after CD11c, Gag p19 and CD86 staining. **Left**: representative experiment. Dashed lines: LPS-exposed MDDCs. Solid black lines: Jurkat-exposed MDDCs, light blue line: Gag $p19^-$ MDDCs. Magenta lines: Gag $p19^+$ MDDCs. **Right**: the same color code is used to represent results from n=15 independent experiments analyzed with one-way ANOVA as described in Supplementary Table 7. **f.** Schematic drawing summarizing the results from Fig. 1 and Supplemental Fig. 2 . The drawing was created using BioRender.com

Figure 2

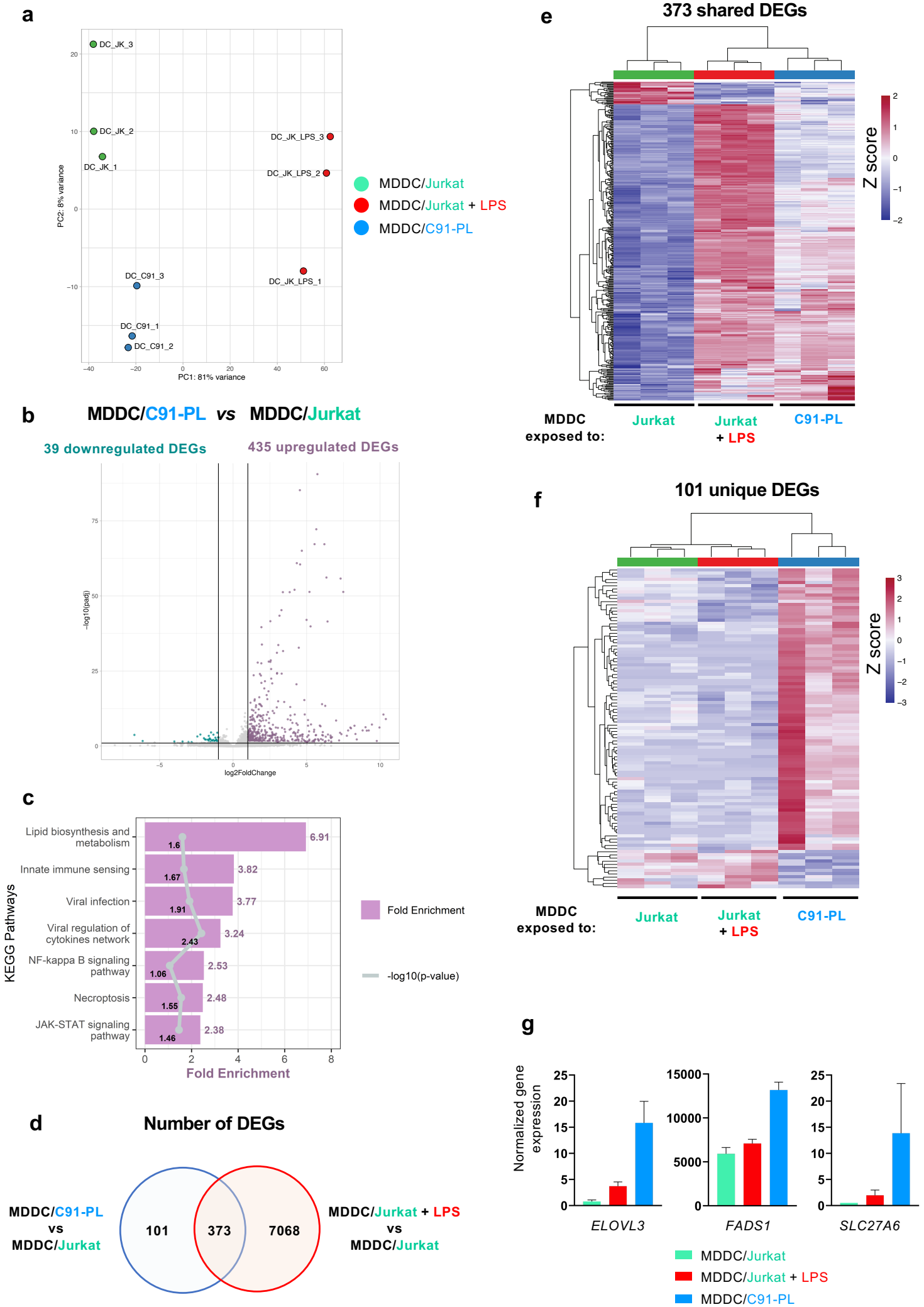
a
DC_JK_3
DC_JK_2
DC_JK_1
DC_JK_LPS_3
DC_JK_LPS_2
DC_JK_LPS_1
DC_C91_3
DC_C91_1
DC_C91_2
PC2: 8% variance
PC1: 81% variance
MDDC/Jurkat
MDDC/Jurkat + LPS
MDDC/C91-PL
b
MDDC/C91-PL vs MDDC/Jurkat
39 downregulated DEGs
435 upregulated DEGs
-log10(padj)
log2FoldChange
c
Lipid biosynthesis and metabolism
Innate immune sensing
Viral infection
Viral regulation of cytokines network
NF-kappa B signaling pathway
Necroptosis
JAK-STAT signaling pathway
KEGG Pathways
Fold Enrichment
-log10(p-value)
d
Number of DEGs
MDDC/C91-PL vs MDDC/Jurkat
101
373
7068
MDDC/Jurkat + LPS vs MDDC/Jurkat
e
373 shared DEGs
Z score
MDDC exposed to:
Jurkat
Jurkat + LPS
C91-PL
f
101 unique DEGs
Z score
MDDC exposed to:
Jurkat
Jurkat + LPS
C91-PL
g
Normalized gene expression
ELOVL3
FADS1
SLC27A6
MDDC/Jurkat
MDDC/Jurkat + LPS
MDDC/C91-PL

Figure 2. Exposure to HTLV-1-infected T cells induces a unique transcriptional signature in MDDCs. MDDCs were cocultured for 24h with control Jurkat cells, or with HTLV-1-infected C91-PL cells, or with control Jurkat cells in the presence of LPS. Cells were then separated and RNA-seq analysis was performed on MDDCs in 3 independent replicates. **a.** Principal component analysis of global similarities in gene expression between samples (DC_ JK: MDDCs after coculture with Jurkat cells, green; DC_JK_LPS: MDDCs after coculture with Jurkat cells in the presence of LPS, red; DC_C91: MDDCs after coculture with C91-PL cells, blue). **b.** Volcano plot of DEGs between MDDCs exposed to C91-PL and MDDCs exposed to Jurkat cells. **c.** KEGG pathways analysis performed on the 435 upregulated DEGs. Bars represent the fold-enrichments, while dots represent the p-values expressed as log10 for each pathway, or their respective mean for grouped pathways (see Supplemental Table 2). **d.** Venn diagram of the DEGs in C91-PL-exposed MDDCs compared to Jurkat-exposed MDDCs (blue circle), and of the LPS-modulated DEGs in Jurkat-exposed MDDCs (red circle). **e-f.** Heatmap of the 373 shared (**e**) and 101 unique (**f**) DEGs. Gene expression was normalized per row. **g.** DESeq2 normalized counts for *ELOVL3*, *FADS1*, and *SLC27A6* across samples.

Figure 3

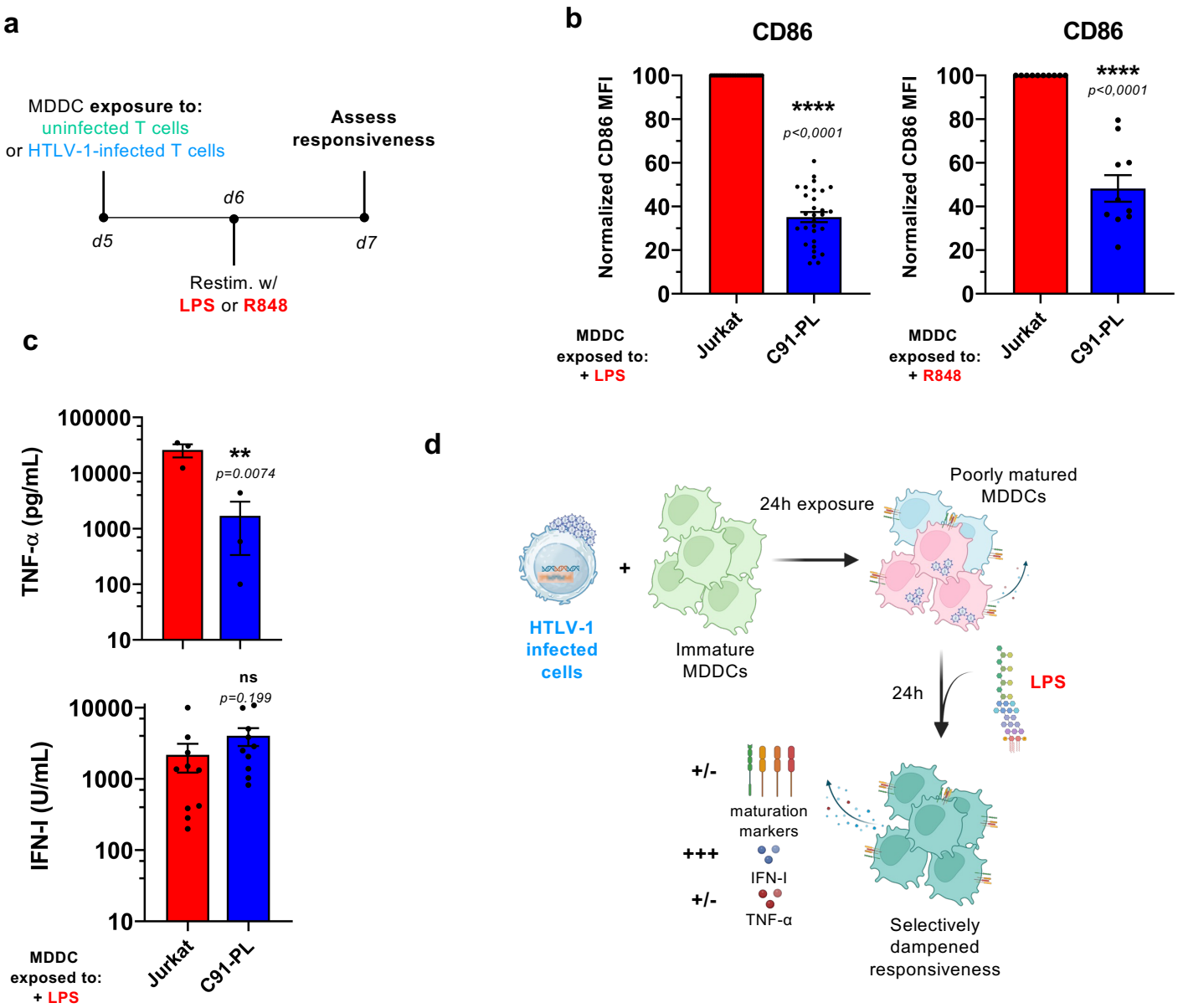

Figure 3. Pre-exposure to HTLV-1-infected T cells dampens the responsiveness of MDDCs to subsequent stimulation. a. Schematic representation of the experimental setting. MDDCs were exposed to uninfected (Jurkat, green) or HTLV-1-infected T cells (C91-PL, blue) for 24h, before restimulation with LPS or R848 for an additional 24h. **b.** Flow cytometry analysis after CD11c and CD86 staining, in LPS- (**left**) or R848-restimulated MDDCs (**right**) pre-exposed to Jurkat (red) or C91-PL (dark blue) cells. Data are represented as the normalized MFI of CD86, with the MFI in restimulated Jurkat-pre-exposed MDDCs set to 100 (n=30 or 10 independent experiments, respectively). Presented data are a subset of Supplementary Figure 5a or 5d, respectively and were analysed with Kruskal-Wallis test or ordinary one-way ANOVA, respectively as described in Supplementary Table 7&8 **c.** Supernatant from the indicated cocultures was collected after LPS restimulation, and TNF-α (**left**) and IFN-I (**right**) concentrations were quantified for n=3 or 10 independent experiments, respectively. Presented data are a subset of Supplementary Figure 5e and were analysed with RM one-way ANOVA or ordinary one-way ANOVA, respectively as described in Supplementary Table 7&8. **d.** Schematic drawing summarizing the results from Fig. 2 and Supplemental Fig. 5. The drawing was created using BioRender.com.

Figure 4

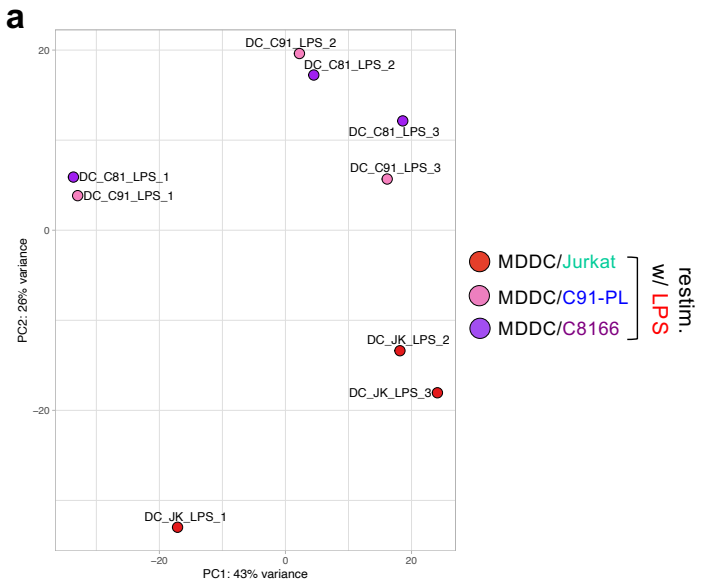
a
DC_C91_LPS_2
DC_C81_LPS_2
DC_C81_LPS_3
DC_C91_LPS_3
DC_C81_LPS_1
DC_C91_LPS_1
DC_JK_LPS_2
DC_JK_LPS_3
DC_JK_LPS_1
PC2: 26% variance
PC1: 43% variance
MDDC/Jurkat
MDDC/C91-PL
MDDC/C8166
restim. w/ LPS

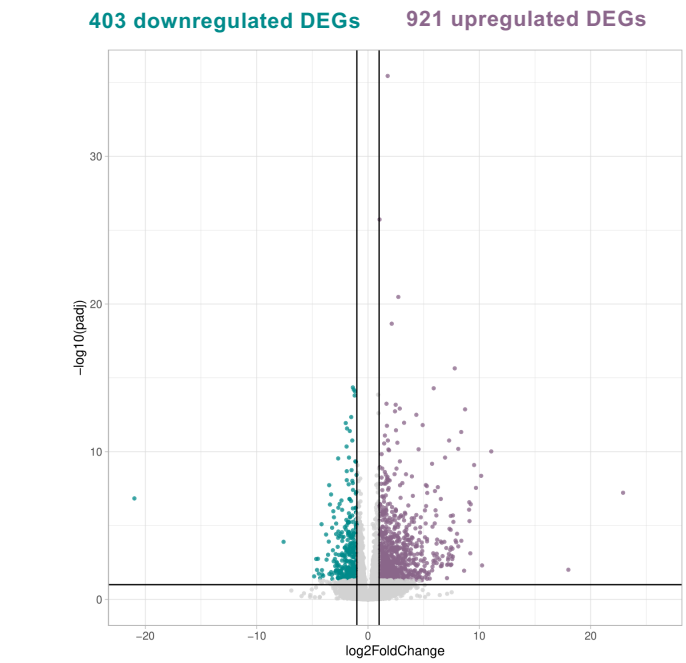
b
MDDC/C91-PL restim. w/ LPS
vs
MDDC/Jurkat restim. w/ LPS
403 downregulated DEGs
921 upregulated DEGs
-log10(padj)
log2FoldChange

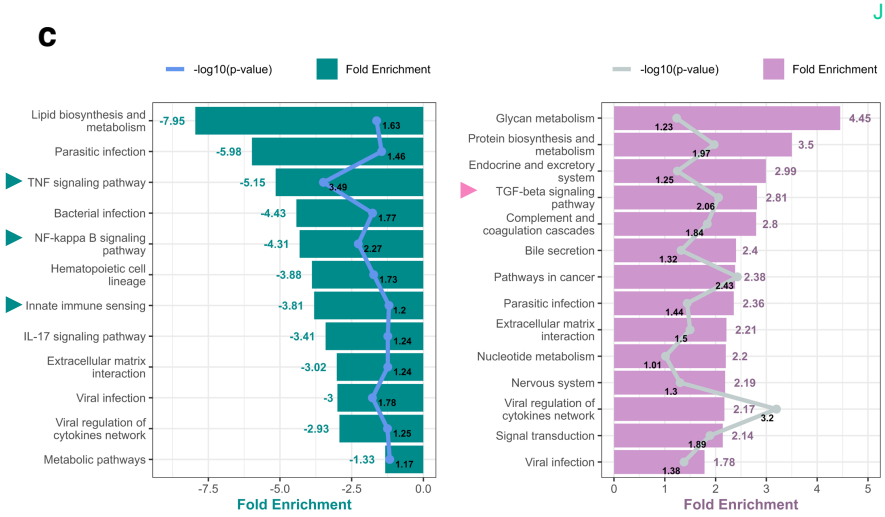
c
-log10(p-value)
Fold Enrichment
Lipid biosynthesis and metabolism
Parasitic infection
TNF signaling pathway
Bacterial infection
NF-kappa B signaling pathway
Hematopoietic cell lineage
Innate immune sensing
IL-17 signaling pathway
Extracellular matrix interaction
Viral infection
Viral regulation of cytokines network
Metabolic pathways
Fold Enrichment
Glycan metabolism
Protein biosynthesis and metabolism
Endocrine and excretory system
TGF-beta signaling pathway
Complement and coagulation cascades
Bile secretion
Pathways in cancer
Parasitic infection
Extracellular matrix interaction
Nucleotide metabolism
Nervous system
Viral regulation of cytokines network
Signal transduction
Viral infection
Fold Enrichment

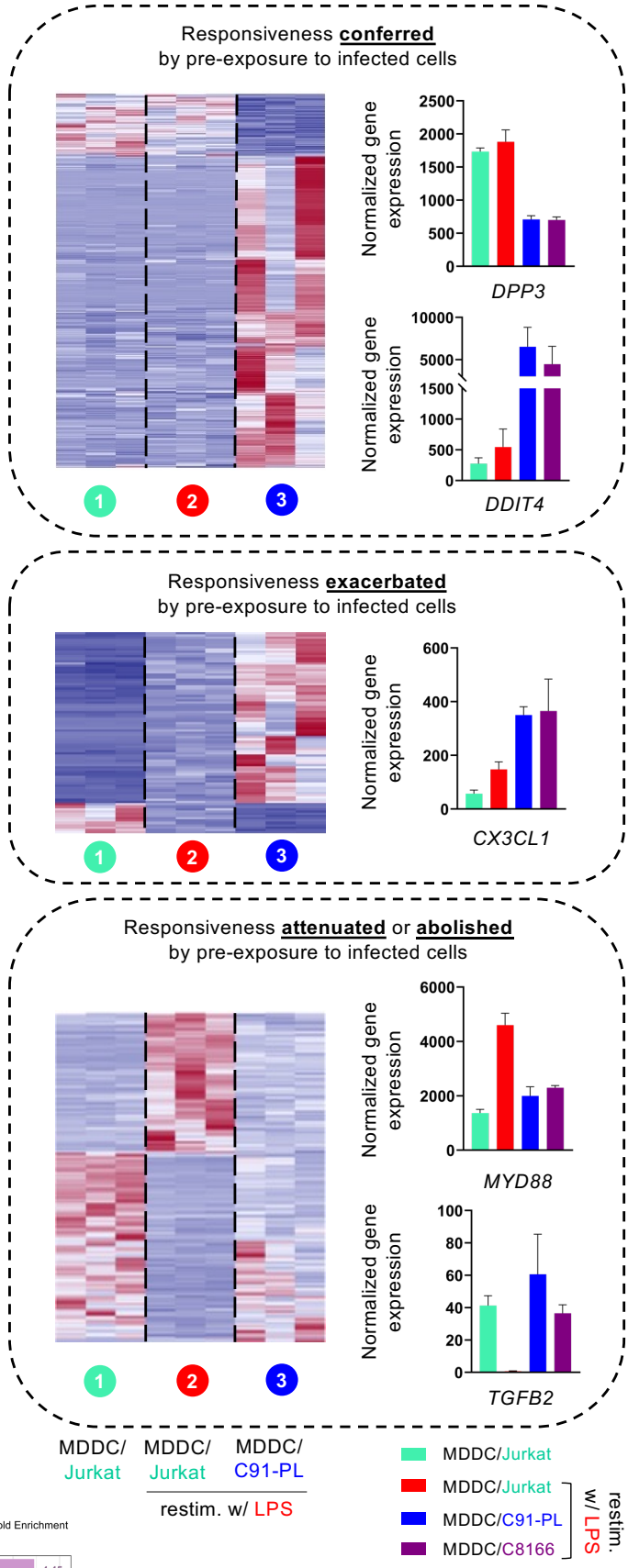
d
Responsiveness conferred
by pre-exposure to infected cells
Normalized gene expression
DPP3
DDIT4
Responsiveness exacerbated
by pre-exposure to infected cells
CX3CL1
Responsiveness attenuated or abolished
by pre-exposure to infected cells
MYD88
TGFB2
MDDC/ Jurkat
MDDC/ Jurkat
MDDC/ C91-PL
restim. w/ LPS
MDDC/Jurkat
MDDC/Jurkat
MDDC/C91-PL
MDDC/C8166
restim. w/ LPS

Figure 4. Pre-exposure to HTLV-1-infected T cells alters the transcriptional response of MDDCs to subsequent stimulation. MDDCs were cocultured for 24h with Jurkat cells, or with HTLV-1-infected C91-PL or C8166 cells, before restimulation with LPS for an additional 24h. Cells were then separated and RNA-seq analysis was performed on MDDCs in 3 independent replicates. **a.** Principal component analysis of global similarities in gene expression between samples (DC_JK_LPS: Jurkat-pre-exposed MDDCs after LPS restimulation, red; DC_C91_LPS: C91-PL-pre-exposed MDDCs after LPS restimulation, pink, DC_C81_LPS: C8166-pre-exposed MDDCs after LPS restimulation, purple). **b.** Volcano plot of DEGs between C91-PL-pre-exposed MDDCs after LPS restimulation, and Jurkat-pre-exposed MDDCs after LPS restimulation. **c.** KEGG pathways analysis performed on the 403 downregulated DEGs (**left**) or on the 921 upregulated DEGs (**right**). Bars represent the fold-enrichments, while dots represent the p-values expressed as log10 for each pathway, or their respective mean for grouped pathways. **d.** Heatmaps and DESeq2 normalized counts across samples of illustrative genes, showing expression across samples of genes belonging to the "conferred" (**top**), "exacerbated" (**middle**) or "attenuated or abolished" (**bottom**) responsiveness pattern.

Figure 5

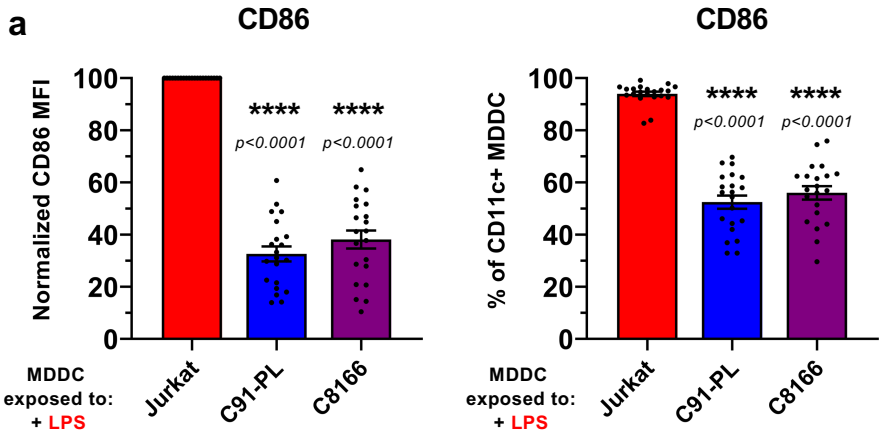

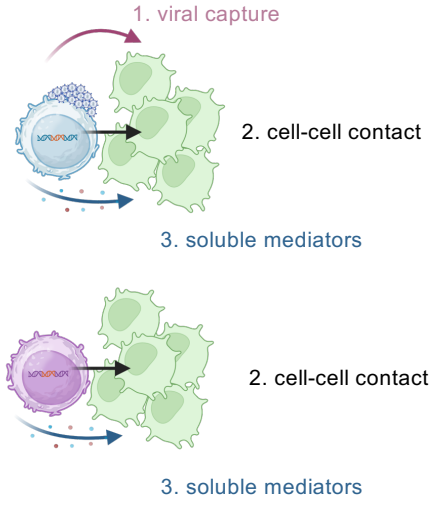

No significant difference:
when cell-cell contacts are possible, the contribution of viral capture is negligible

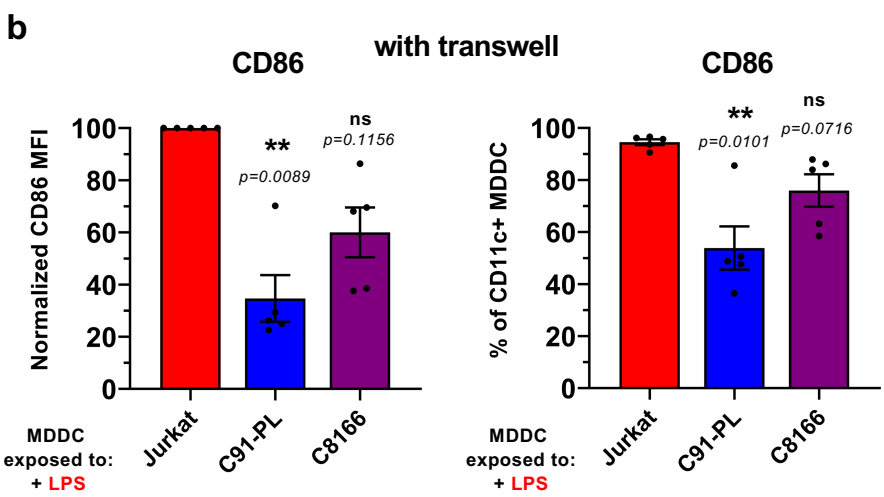

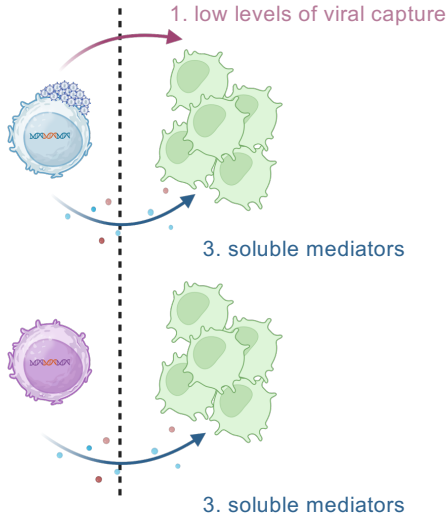

Difference:
When cell-cell contacts are not possible, the contribution of viral capture is detectable

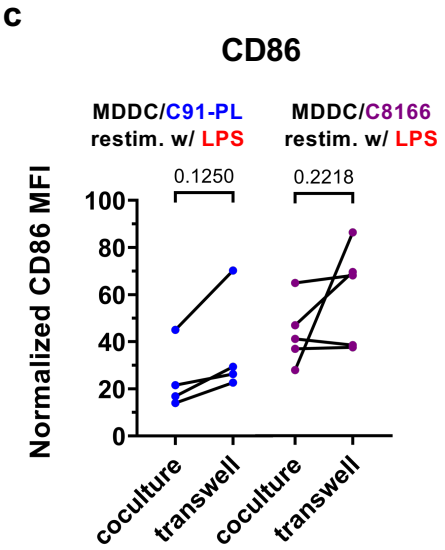

Figure 5. Neither HTLV-1 viral capture, nor cell-cell contact with infected T cells, are strictly required to dampen the responsiveness of MDDCs to subsequent stimulation. a-b. MDDCs were cocultured for 24h with Jurkat cells, or with HTLV-1-infected C91-PL or C8166 cells, in the absence (**a**) or presence (**b**) of a transwell insert (0.4µm pore diameter), before re-stimulation with LPS for an additional 24h. Flow cytometry analysis after CD11c and CD86 staining. Data are represented as the normalized MFI of CD86, with the MFI in re-stimulated Jurkat-exposed MDDCs set to 100 (**left**), or as the percentage of $CD86^+$ MDDCs (**right**), and summarize n=21 (**a**) or n=5 (**b**) independent experiments. Red: Jurkat-exposed MDDCs restimulated with LPS; dark blue: C91-PL pre-exposed MDDCs restimulated with LPS; purple: C8166 pre-exposed MDDCs restimulated with LPS. Detailed statistical analysis is presented in Supplementary Table 7. Briefly, the statistical difference between means was tested using RM one-way ANOVA (a, left and b, right) or Friedman test (a, right and b, left), in accordance with the distribution. **c.** Paired percentage of $CD86^+$ MDDCs in standard coculture (as measured in **a**), or with a transwell insert (as measured in **b**), with HTLV-1-infected C91-PL (**left**) or C8166 cells (**right**). Data summarized n=4 or 5 independent experiments, respectively analysed with paired t-test or its non parametric equivalent Wilcoxon matched-pairs signed rank test as described in Supplementary Table 7. **d.** Schematic drawing summarizing the results from Fig. 5 and Supplemental Fig. 8. The drawing was created using BioRender.com.

Figure 6

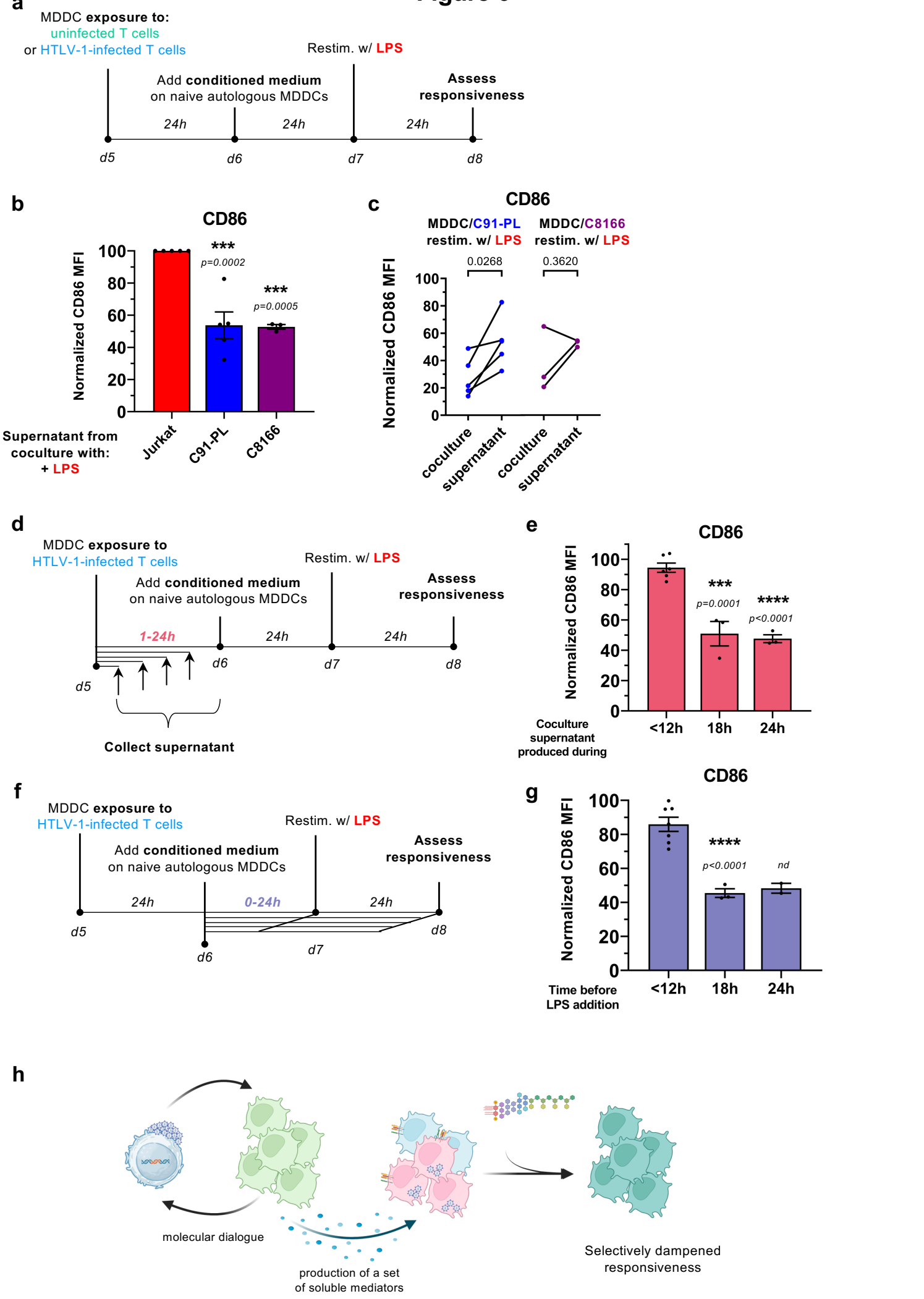
a
MDDC exposure to:
uninfected T cells
or HTLV-1-infected T cells
Restim. w/ LPS
Add conditioned medium
on naive autologous MDDCs
Assess
responsiveness
24h
24h
24h
d5
d6
d7
d8
b
CD86
Normalized CD86 MFI
100
80
60
40
20
0
***
p=0.0002
***
p=0.0005
Supernatant from
coculture with:
+ LPS
Jurkat
C91-PL
C8166
c
CD86
MDDC/C91-PL
restim. w/ LPS
MDDC/C8166
restim. w/ LPS
0.0268
0.3620
Normalized CD86 MFI
100
80
60
40
20
0
coculture
supernatant
coculture
supernatant
d
MDDC exposure to
HTLV-1-infected T cells
Restim. w/ LPS
Add conditioned medium
on naive autologous MDDCs
Assess
responsiveness
1-24h
24h
24h
d5
d6
d7
d8
Collect supernatant
e
CD86
Normalized CD86 MFI
100
80
60
40
20
0
***
p=0.0001
****
p<0.0001
Coculture
supernatant
produced during
<12h
18h
24h
f
MDDC exposure to
HTLV-1-infected T cells
Restim. w/ LPS
Add conditioned medium
on naive autologous MDDCs
Assess
responsiveness
24h
0-24h
24h
d5
d6
d7
d8
g
CD86
Normalized CD86 MFI
100
80
60
40
20
0
****
p<0.0001
nd
Time before
LPS addition
<12h
18h
24h
h
molecular dialogue
production of a set
of soluble mediators
Selectively dampened
responsiveness

Figure 6. A molecular dialogue between HTLV-1-infected T cells and MDDCs induces the release of soluble tolerogenic mediators. a. Schematic representation of the experimental setting. MDDCs were cocultured for 24h with uninfected Jurkat cells, or with HTLV-1-infected C91-PL or C8166 cells. Conditioned medium was collected and added on naive autologous MDDCs for 24h, before restimulation with LPS for an additional 24h. **b.** Flow cytometry analysis after CD11c and CD86 staining. Data are represented as the normalized MFI of CD86, with the MFI in re-stimulated MDDCs cultured in MDDC/Jurkat-conditioned medium set to 100. The color code is the same as in Fig. 5. Data summarize n=5 (C91-PL) or n=3 (C8166) independent experiments analysed with ordinary one-way ANOVA as described in Supplementary Table 7. **c.** Analysis of paired experiments, after standard coculture with C91-PL (**left**) or C8166 cells (**right**, as measured in **Fig. 5a**), or after culture in conditioned medium from MDDC/C91-PL coculture or from MDDC/C8166 coculture (n=5 or 3 independent experiments, respectively). Data were analysed with Paired t-test as described in Supplementary Table 7. **d.** Schematic representation of the experimental setting. MDDCs were cocultured with C91-PL, and conditioned medium was collected at multiple time points of coculture and added on naïve autologous MDDCs for 24h, before re-stimulation with LPS for another 24h. **e.** Flow cytometry analysis after CD11c and CD86 staining. Data are represented as the normalized MFI of CD86, with the MFI in LPS-stimulated MDDCs cultured in normal medium set to 100 (n=6 and n=3 independent experiments, for <12h and for 18h and 24h conditions, respectively). Data were analysed with ordinary one-way ANOVA as described in Supplementary Table 7. **f.** Schematic representation of the experimental setting. MDDCs were cocultured for 24h with C91-PL. Conditioned medium was collected and added on naive autologous MDDCs for the indicated time, before re-stimulation with LPS for another 24h. **g.** Flow cytometry analysis after CD11c and CD86 staining. Data are represented as the normalized MFI of CD86, with the MFI in LPS-stimulated MDDCs cultured in normal medium set to 100 (independent experiments were performed using n=7 for <12h condition, n=3 for 18h condition and n=2 for 24h condition). Statistical analysis of the two first columns was performed with Unpaired Welch's t-test. **h.** Schematic drawing summarizing the results from Fig. 6 and Supplemental Fig. 9. The drawing was created using BioRender.com.